

1
2
3
4
5
6
7
8
9
10
11
12
13
14
15
16
17
18
19
20
21
22
23
24
25
26
27

The Mediterranean and Black Sea meteotsunamis: An overview

Ivica Vilibić^{1}, Cléa Denamiel¹, Petra Zemunik¹, Sebastian Monserrat²*

¹ Institute of Oceanography and Fisheries, Šetalište I. Meštrovića 63, 21000 Split, Croatia

² Department of Physics, University of the Balearic Islands, Palma de Mallorca, Spain

Correspondence to: I. Vilibić, vilibic@izor.hr

Submitted to Natural Hazards special issue on meteotsunamis

April 2020

28 **Abstract**

29

30 This paper presents the first comprehensive review of the Mediterranean and Black
31 Sea meteorological tsunamis or meteotsunamis (atmospherically induced destructive long
32 ocean waves in the tsunami frequency band) based on the available literature, tools and
33 services. The Mediterranean and Black Seas are micro-tidal basins; therefore, rapid sea level
34 changes in the tsunami frequency band may strongly affect coastal regions and infrastructures
35 and endanger human lives. The review also includes a succinct bibliography of Mediterranean
36 and Black Sea meteotsunami papers and evaluates their structure in respect to geographical
37 extent, the type of tools used (observations versus modelling), and source processes in the
38 atmosphere versus ocean manifestations. This review continues with a presentation of major
39 meteotsunami events and a discussion about their sources, the resonant transfer of energy
40 towards the sea, their propagation towards shore and their interactions with bathymetry.
41 Meteotsunami monitoring and forecasting systems are overviewed with respect to available
42 observations, deterministic and stochastic modelling tools and operational early warning
43 networks. This review includes an important assessment of operational and research gaps and
44 ideas for improving research tools and understanding of various aspects of meteotsunamis.
45 The authors believe and hope that this review will help researchers and services to increase
46 or improve their capacities and skills for conducting better research on meteotsunamis, not
47 just in the Mediterranean and Black Seas, but in all ocean basins around the world affected by
48 this destructive and dangerous phenomenon.

49

50 **Key words:** Meteotsunamis; Review; Mediterranean; Black Sea

51

52

53 1. Introduction

54

55 Since ancient times, meteorological tsunamis or meteotsunamis – atmospherically
56 induced destructive long ocean waves in the tsunami frequency band – have been known to
57 impact coastal communities (Monserrat et al. 2006; Pattiaratchi and Wijeratne 2015; Vilibić
58 et al. 2016; Rabinovich 2020). In several cases, memorable events even gave birth to local
59 legends, for example, that of Vrboska Bay (Hvar Island, Adriatic Sea). There, after a procession
60 was hit by a meteotsunami (Šepić and Orlić 2020), the coastal communities united. The Arabs
61 landed in Mazarra del Vallo (southwestern Sicily coast) in the 9th century and named the local
62 river Mazaro (“possessed”) due to the propagation of a meteotsunami bore (Šepić et al.
63 2018a). Since then, impacts by meteotsunamis have been recorded in a large number of
64 coastal communities in all continents of the world except Antarctica. In addition, a variety of
65 local names have been used for the phenomenon: *rissaga* in the Balearic Islands (Ramis and
66 Jansà 1983; Monserrat et al. 1991a 1991b), *marrobbio* (*marrubbio*) in the Strait of Sicily
67 (Colucci and Michelato 1976; Candela et al. 1999), *milghuba* in the Maltese Islands (Drago
68 2009), *šćiga* (*štiga*) in the Adriatic Sea (Hodžić 1979/1980, Orlić, 1980), *abiki* in Japan (Honda
69 et al. 1908; Nakano and Unoki 1962; Hibiya and Kajiura 1982), and *Seebär* in the Baltic Sea
70 (Defant 1961; Metzner et al. 2000; Pellikka et al. 2014). In addition to locations with existing
71 local names for meteotsunamis, which presumably reflect the destructiveness of the past
72 meteotsunami events, there are a great number of additional places where severe
73 meteotsunami events occurred: the English Channel and UK coast (Proudman 1929; Haslett
74 et al. 2009; Williams et al. 2019), the Great Lakes (Ewing et al. 1954; Bechle et al. 2016), the
75 East US Coast, from Florida to Maine (Churchill et al. 1995; Šepić and Rabinovich 2014; Vilibić
76 et al. 2014c; Wertman et al. 2014), the US and Canadian West Coast (Thomson et al. 2009),
77 the Patagonian Shelf (Dragani et al. 2014), the South African coast (Okal et al. 2014), the
78 Australian shelf (Pattiaratchi and Wijeratne 2014) and many other locations.

79 Occasionally, meteotsunamis are characterized by sea level oscillations of several
80 metres with periods from several minutes to an hour. Furthermore, meteotsunami events can
81 cause human losses and injuries (e.g., the 1954 and 2003 events in the Great Lakes – Ewing et
82 al. 1954; Linares et al. 2019; the 1979 Nagasaki Bay abiki – Hibiya and Kajiura 1982; the 2017
83 Dayyer meteotsunami in the Persian Gulf – Salaree et al. 2018; and the 2014 Odessa
84 meteotsunami – Šepić et al. 2018b) in addition to frequent, and sometime substantial, coastal

85 infrastructure damage (Pattiaratchi and Wijeratne 2015). Still, the destruction and property
86 damage caused by meteotsunamis has been restricted to certain hot spots (harbours, bays,
87 beaches) and is much lower than that resulting from destructive seismic tsunamis due to the
88 smaller wave heights and spatial extent of meteotsunamis as compared to largest tsunamis.
89 In addition, human casualties from meteotsunamis are rare and occur during the most
90 extreme meteotsunami events, while such casualties can be substantial during strong seismic
91 tsunamis, in particular in those generating ocean-wide impacts (Gusiakov et al. 2019).

92 Because of the destructive nature of meteotsunamis, which can occur without warning
93 even during 'calm' weather, researchers have studied the physics of such events and their
94 generation and propagation/growth towards the shore. The most intriguing question, related
95 to how energy is transferred from the atmosphere to the meteotsunami waves, was explained
96 in 1929 as a resonance mechanism: the so-called *Proudman resonance* (Proudman 1929).
97 Namely, atmospheric disturbances with high-frequency (from minutes to hours) energy,
98 which can sometime be seen on old barogram records, may travel over shelf areas at the
99 speed of tsunami waves (i.e., $U \approx (gH)^{1/2}$, where U is the speed of the atmospheric disturbance,
100 H is the water depth and g is gravity). If such conditions persist, the amplification of the wave
101 that is generated is multiplied (Rabinovich 2009). However, in real shelf areas, the varying
102 bathymetry, tides and currents are known to affect the strength of the resonance (Williams et
103 al. 2020), which can differ from the theoretical conditions described for flat bathymetries.
104 Travelling atmospheric disturbances may generate edge waves on sloping bathymetries near
105 a shore (so-called Greenspan resonance, Greenspan 1956) or may generate shelf waves
106 directly on shelves of limited size (Rabinovich 1993). Compared to tsunami waves,
107 meteotsunami waves are constantly modified by the force of the atmosphere during their
108 travel towards the shoreline (e.g., Hibiya and Kajiura 1982), while the bathymetry
109 simultaneously changes their properties. The waves can reach destructive levels along open
110 sea beaches, such as was observed during the Daytona Beach meteotsunami of 3 July 1992,
111 when wave heights reached 3 m above tide (Churchill et al. 1995). If the waves impact bays or
112 harbours, they can be further amplified through the harbour resonance (Wilson 1972;
113 Rabinovich 2009) and reach heights of up to 6 m, such as occurred during the Great Vela Luka
114 flood of 21 June 1978 (Vučetić et al. 2009; Orlić et al. 2010).

115 Specific atmospheric conditions that lead to intense, long-lived and fast atmospheric
116 disturbances have also been investigated as mechanism of generating meteotsunami events.

117 Physical mechanisms responsible for keeping energy near the sea surface over hundreds or
118 more kilometres are needed to reach a substantial amplification of the meteotsunami waves.
119 There are several atmospheric processes found to satisfy these conditions. Wave ducting of
120 internal gravity waves appears to commonly accompany meteotsunamis in the Mediterranean
121 and other mid-latitude locations (Monserrat and Thorpe 1996; Tanaka 2010; Šepić et al.
122 2015a). Other processes in the world oceans include wave-CISK (Convective Instability of the
123 Second Kind, Belušić et al. 2007), squall lines and derechos (Ewing et al. 1954; Churchill et al.
124 1995; Paxton and Sobien 1998; Šepić and Rabinovich 2014), mesoscale convective storms
125 (Linares et al. 2019; Williams et al. 2020), and rain bands in tropical cyclones (Shi et al. 2020).
126 However, the capacity to reproduce the generation and propagation of meteotsunamigenic
127 atmospheric instabilities, including their interaction with orography, are at the edge of the
128 state-of-the-art atmospheric numerical model capacities (Renault et al. 2011; Horvath and
129 Vilibić 2014; Denamiel et al. 2019a) due to both the physics implemented and the coarse
130 resolution.

131 In recent decades, through the increased availability of high-frequency (1 min) sea level
132 and meteorological data and the development of numerical tools accompanied by the
133 increase in high-performance computing resources, the physics of meteotsunami waves and
134 their atmospheric sources have been increasingly researched (Vilibić et al. 2016).

135 Meteotsunamis are a worldwide phenomenon; however, literature reviews show that
136 they have been traditionally studied much more in the Mediterranean than in the rest of the
137 world. This can be explained by the micro-tidal nature of the Mediterranean Sea where tidal
138 amplitudes (a few tens of centimetres except in the Gulf of Gabes and the northern Adriatic
139 Sea, Tsimplis et al. 1995; Medvedev et al 2020) are an order of magnitude smaller than the
140 amplitudes of meteotsunamis. In consequence, coastal infrastructure along the
141 Mediterranean coast is generally not adapted to accommodate rapid sea level changes,
142 resulting in much greater damage and flooding during meteotsunami events than what occurs
143 along macro-tidal coasts of the world (Fig. 1).

144 The first theoretical explanation for Mediterranean meteotsunamis was provided at
145 the beginning of the 20th century for the Balearic/Catalan region where Fontserè (1934)
146 noticed the coincidence between rapid changes in the air pressure and seiches in the
147 Barcelona harbour. Almost simultaneously, Caloi (1938) investigated air pressure and sea level
148 records in the northern Adriatic and associated the recorded seiches with propagating

149 atmospheric disturbances. Subsequently, in late 1970s and early 1980s, research on rissaga
150 (i.e., meteotsunami) events occurring in Ciutadella (Balearic Islands) demonstrated their
151 relationship with specific synoptic conditions (Ramis and Jansà 1983). These observations
152 were the basis for the subsequent rissaga synoptic forecasting system, which tracked (i)
153 ground and low (below 850 hPa) level atmosphere conditions in which a weak cyclone was
154 present during rissaga events, (ii) south-westerly flow of dry and warm African air at levels
155 corresponding to approximately 850 hPa, which are situated over a relatively cold surface air
156 and give rise to a characteristic temperature inversion, (iii) the strong south-westerly air flow
157 over the Western Mediterranean that occurs at 500 hPa, and (iv) a jet stream between the
158 Balearic Islands and the Iberian Peninsula, which occurs at 300 hPa.

159 In the Adriatic Sea, the Great Flood of Vela Luka on 21 June 1978 (Vučetić et al. 2009)
160 triggered extensive research on the origin of this event. Several active theories to explain the
161 observed waves were developed: (i) a tsunami triggered by the 6.4 Mw Aegean earthquake,
162 which took place the day before (Zore-Armanda, 1979; however, no correspondence between
163 the observed and theoretical arrival times of tsunami waves has been found, and the distance
164 between the epicentre and Vela Luka is far too large; (ii) a tsunami triggered by a landslide
165 along the Italian side of the Middle Adriatic Pit (Bedosti 1980); however, no waves were
166 reported close to the source, which would be expected for landslide tsunamis; (iii) cyclonic-
167 waves generated by a cyclone in the open sea that propagated as free waves toward the
168 affected bays (Hodžić 1979/1980); however, no energy transfer mechanism has been
169 proposed; and (iv) a resonant transfer of energy from intense air pressure disturbances that
170 propagated north-eastward at a speed of 22 m/s in addition to long ocean waves generated
171 through the Proudman resonance (Orlić 1980); the latter was confirmed by recent
172 investigations (Orlić et al. 2010), although a mismatch concerning the speed of the air
173 disturbance and the effect of the Proudman resonance versus other effects driven by
174 bathymetry, was found.

175 Since these early studies, the science of the Mediterranean meteotsunamis has
176 substantially progressed; this progress was initiated by major meteotsunami events for which
177 observations were available: those that occurred in the 1980s and 1990s in the Balearic Islands
178 (Tintoré et al. 1988) and in the 2000s in the Adriatic Sea (Vilibić and Šepić 2009). An extensive
179 application of numerical modelling tools followed these observations, peaking in the 2010s
180 with the development of high-performing computing facilities (Orlić et al. 2010; Renault et al.

181 2011). Investigations of atmospheric sources, energy transfer towards the sea, and the
182 propagation and amplification of meteotsunami waves have been the main topics of these
183 investigations. A comprehensive and systematic overview of the knowledge acquired in these
184 papers is the primary motivation for this study, which is the first such study dedicated to the
185 Mediterranean Sea (including the Black Sea). Section 2 introduces the topic through an
186 overview of the media coverage and societal behaviour that occurred after major
187 meteotsunami events, including the reaction of society, which is different in various countries.
188 Section 3 contains a basic map of the Mediterranean and Black Sea meteotsunami papers cited
189 by the Web of Science database, which includes the geographical coverage, tools used in the
190 research and the atmosphere or ocean meteotsunami source. Section 4 gives an overview of
191 meteotsunami research, from that pertaining to the mechanism of atmospheric generation to
192 the genesis and amplification of meteotsunami waves in coastal regions. Existing
193 meteotsunami monitoring and forecast systems in the Mediterranean and Black Seas,
194 including observations, deterministic models, stochastic approaches, and hazard assessments
195 are presented in Section 5. Section 6 describes the major bottlenecks that exist in
196 Mediterranean and Black Sea meteotsunami research, followed by perspectives on future
197 research and research directions and conclusions described in Section 7.

198

199 **2. Description, media coverage and societal behaviour after major meteotsunami events**

200

201 In recent decades, major meteotsunami events associated with structural damage in
202 coastal regions that have impacted local populations have often attracted local and national
203 media attention. In this section, three examples of media coverage and societal behaviour
204 during and after Mediterranean and Black Sea meteotsunamis will be briefly overviewed.

205

206 *2.1. The Great Vela Luka Flood of 21 June 1978*

207

208 This event, characterized by wave heights up to 6-m in the city of Vela Luka (Korčula
209 Island, Croatia), impacted the whole middle Adriatic from the Italian to the Croatian coasts
210 and is often referred to in the literature as the most devastating and memorable
211 meteotsunami in the Adriatic. The Vela Luka Bay is funnel shaped and has been known by local
212 inhabitants to have persistent eigen oscillations that normally reach less than a metre or two

213 in height and can be easily handled by the city harbour without suffering inundation or
214 structural damage (Orlić 2015). This destructive event was described in detail by Vučetić et al.
215 (2009), while a collection of newspaper articles and other relevant material was documented
216 by Vučetić and Barčot (2008). The event attracted a large amount of media attention, while
217 scientists tried to explain the physical mechanisms.

218 The first meteotsunami waves were observed in the early morning, on 21 June 1978 at
219 4:15 UTC (local time 5:15), overtopping the piers and quays and flooding houses at the
220 waterfront. Intuitively, the electricity service switched off the power for the whole city to
221 prevent any human losses and damage caused by electric shocks. Telephone connections
222 were also disabled during and after the event. The sea oscillated every 15-20 min, peaking at
223 7:00 UTC, when a 6-m wave was observed at the top of the harbour (in fact, several media
224 sources reported wave heights of 8 to 11 m, as no data were available to quantify the trough
225 of the meteotsunami wave that emptied the harbour). The sea returned to calm at
226 approximately 10:00 UTC, leaving a great amount of household goods floating within the bay,
227 between sunk boats and ships, with heavy furniture (e.g., refrigerators) removed from several
228 houses and a health centre destroyed at the top of the bay.

229 The media reported the event the very first day, providing basic facts and impact
230 assessments (Vučetić and Barčot 2008): *“Life in Vela Luka is paralyzed. People were not on*
231 *their jobs today. All of Vela Luka is on its feet this morning from five o'clock. The Vis ferry did*
232 *not dock at all, but carried forward towards Split. The city was run out of food and telephone*
233 *connections. The gasoline station was also destroyed. It is unknown at this time how many*
234 *boats, ships and cars were damaged. The level of destruction is enormous and it is impossible*
235 *to talk about it now ... Military units from the island area also came to the rescue, and police*
236 *is having a great trouble regulating traffic that is completely paralyzed.”*

237 Simultaneously, after the first impact, the local authorities started to organize cleaning
238 of the bay and announced rules of behaviour via a public proclamation on the day after the
239 event (Fig. 2). These rules, designed to mitigate damage and prevent uncontrolled behaviour
240 of the population, included: (i) the treatment of water, in particular the potable water, (ii) the
241 treatment of the food stored in houses, (iii) the treatment of vegetables in gardens, (iv) the
242 recovery of flooded basements and houses, (v) the control of personal hygiene and the
243 management of pre-existing health conditions, and (vi) rules for bathing and swimming. Three
244 days later, the authorities engaged local populations in voluntary sanitation and cleaning of

245 the Vela Luka area, after which the city become safe for living and working. At that time, the
246 final estimation of the damage caused by the meteotsunami was approximately 7 million US
247 dollars, which was approximately a quarter of the annual income of the whole Korčula Island.

248 In the following month, several researchers, such as Tonko Tabain, who is quoted
249 hereafter, were interviewed by the media to provide a theoretical background of the event to
250 the general public: “...*the second hypothesis, by which sea pressure waves are the causative*
251 *cause of šćiga (o.a. meteotsunami), provides an answer to the questions asked ... sea pressure*
252 *waves are generated by atmospheric pressure waves, and these arise when two air masses of*
253 *different density (temperature) move at different speeds relative to each other.”* After the first
254 interviews, more research was carried out and papers on the event by Hodžić (1979/1980)
255 and Orlić (1980) were published. Unfortunately, a comprehensive research program
256 developed in the following two years by the Academy of Science and Arts in Zagreb, which
257 consisted of the installation of a monitoring network and a meteotsunami hazard assessment
258 via numerical models in the Vela Luka area, was never implemented. Interestingly, during this
259 event, reflected waves were far less destructive than those that hit the Croatian coastline,
260 which were also observed with a few hour time lag along the Italian coast (Orlić et al. 2010).
261 As the two shorelines were part of the different political systems (socialism in Yugoslavia
262 versus capitalism in Italy), the explanation for the observed waves was dramatically different:
263 Bedosti (1980) hypothesized that the waves were the result of a submarine landslide along
264 the western flank of the Middle Adriatic Pit. Indeed, such a hypothesis did not include any of
265 the observations available along the Croatian coastline, presumably due to a lack of
266 information available to the Italian researchers. More than 30 years were thus needed to
267 gather all available Italian and Croatian observations and provide reasonable explanations and
268 quantifications of the physical mechanism of the event (Vučetić et al. 2009; Orlić et al. 2010).

269

270 2.2. *The destructive rissaga event of 21 June 1984*

271

272 Meteotsunamis in the Balearic Islands are historically known by the local name of
273 rissaga. The first references of the hazardous effects of rissaga events in Ciutadella (the
274 eastern coast of Menorca island) are found in documents dating to the XV century. The
275 phenomenon is also described in detail by Riudavets as early as 1885 in his book: History of
276 Menorca Island. From then on, many references in local newspapers exist but there are only

277 very few mentions in the scientific literature (Fontseré 1934). Rissaga was not extensively
278 considered by the scientific community until the early eighties, when several works were
279 published in Spanish by Agustí Jansà and Clemente Ramis (Ramis and Jansà 1983; Jansà 1986
280 1987). Several of the pioneering publications were motivated by the extreme event observed
281 in 1984.

282 On 21 June 1984, a singular rissaga event struck Ciutadella harbour. Local eyewitnesses
283 reported that several minutes after four o'clock in the morning (local time) the harbour,
284 located at the end of Ciutadella inlet, suddenly became dry. Shortly after, when water re-
285 entered the inlet, it washed up towards the harbour end most of the boats that previously had
286 broken their mooring ropes, hit each other and caused great damage (Fig. 3). After the initial
287 "big wave", large sea level oscillations (of more than one metre), with a period coinciding with
288 an inlet seiche (approximately 10 min), remained for several hours. Total damage was
289 tremendous: of the 117 boats moored at the port at that time, 81 were affected and 35 were
290 sunk. Most of the local fishing float became inoperative during the following months.
291 Fortunately, no personal injuries were reported, but economic damage was quantified to be
292 over two and a half million euros.

293 Abnormal sea level oscillations, although of much less of a consideration than in
294 Ciutadella, were also observed in other Menorca inlets, such as adjacent Platja Gran. Similar
295 large amplitude sea level oscillations that caused moderate damage were also reported in
296 other harbours on the nearby Mallorca island, such as those in Porto Colom or Porto Cristo.

297 The next day, local newspapers related several witness accounts of how a sudden blow
298 of wind woke them up in the middle of the night. When a short time later they looked towards
299 the port, they were surprised to find the port empty of water. Then, a great wave entered the
300 port and washed away everything in its path. Although rissaga were not a rare phenomenon
301 in Ciutadella, everyone agreed this particular event was one of the more destructive ever
302 experienced at this location.

303 No sea level records were available at the time, but the largest oscillations in Ciutadella
304 were estimated to reach more than 4 m of through-to-crest amplitude. A detailed analysis of
305 this event, including the examination of the atmospheric synoptic situation, vertical structure
306 of the wind and pressure and the available records of surface winds and atmospheric pressure
307 at several stations were provided by Jansà (1986). Most of the generation mechanisms
308 suggested in that work remain valid to this day.

309

310 2.3. The Odessa meteotsunami of 27 June 2014

311

312 This destructive event has been documented as a chain of meteotsunamis that hit the
313 coasts of the Mediterranean and Black Seas and was described in detail and investigated by
314 Šepić et al. (2018b). To summarize, sudden tsunami waves with wave heights of more than 1
315 m (up to 2.5 m as claimed by several eyewitnesses) hit two beaches near Odessa (Ukraine),
316 which were inundated to a distance of 50 m, and resulted in 15 people injured. This extreme
317 event was unprecedented as it occurred during calm weather in a region located far from
318 major earthquake zones (Yalçiner et al. 2004) where seismic tsunamis are not frequent.

319 In addition to the injuries, the meteotsunami generated a wave of panic within the
320 local population, amplified by the unstable political situation during the Ukrainian crisis
321 ([https://en.wikipedia.org/wiki/2014 Odessa clashes](https://en.wikipedia.org/wiki/2014_Odessa_clashes)), which, less than two months before,
322 left 48 people dead (the highest toll since The Great War) during clashes in Odessa. In this
323 context of terror, several maladaptive hypotheses to explain the generation of such extreme
324 waves circulated among the population and were even promoted by the media (e.g.,
325 <https://dumskaya.net/news/nevedomaya-hujnya-037089>): *“Meanwhile, scientists continue
326 to put forward more and more versions of what happened. Most adhere to a version of the
327 anthropogenic or technogenic nature of what happened, they assume that the wave appeared
328 as a result of human activity ... At the same time, eyewitnesses refute the assumption that a
329 large vessel (at least 50 thousand tons displacement) could travel at high speed (more than 30
330 knots) in the immediate vicinity of the coast, which could only cause such a wave. Also unlikely
331 are the versions that the wave was the result of dredging, although today, indeed, a dredger
332 was seen near the Black Sea. Another hypothesis was put forward by the hydrologist Anatoly
333 Petrachenko. He suggested that the cause could be, for example, the explosion of a small boat
334 with ammunition that sank during the Great Patriotic War near Lustdorf ... Firstly, such an
335 explosion would undoubtedly be recorded by seismologists, whose station is 15 km from
336 Chernomorka. Secondly, there were no stunned fish and victims of water hammer at the scene,
337 which puts an end to all the "explosive" versions ... In turn, the inhabitants of Chernomorka
338 argue that such large waves in these places occur every few years and are the result of a
339 complex interaction of warm and cold currents. This time, such a wave was stronger than
340 usual.”*

341 To prove that the observed waves were indeed meteotsunamis, Šepić et al. (2018b)
342 collected all available observations and carried out several numerical experiments. Although
343 the magnitudes of the waves were underestimated, presumably due to insufficient resolution
344 of the atmospheric forcing and the bathymetry at the shelf edge and in coastal regions used
345 in the study, the authors reproduced the spatial extent of the event and indicated that it was
346 caused by remote generation of long ocean waves that are topographically directed towards
347 the affected beaches.

348

349 **3. Succinct analysis of the Mediterranean meteotsunami bibliography**

350

351 The bibliography of the Mediterranean and Black Sea meteotsunamis (presented in
352 Fig. 4a) is composed of 55 research papers, as archived by the Web of Science (WoS) database
353 from 1955 to 2019. The bibliography encompasses both well-researched hot spots for
354 meteotsunamis for which many papers have been published, such as the Balearic Islands or
355 the Adriatic Sea, as well as sites that contain a single meteotsunami observation, such as the
356 Black Sea sites. The first article on the list, by Tintoré et al. (1988), was preceded by a great
357 number of non-WoS papers that mostly described different aspects of the Balearic and
358 Adriatic meteotsunamis (Fontseré 1934; Caloi 1938; Colucci and Michelato 1976; Hodžić
359 1979/1980; Orlić 1980; Ramis and Jansà 1983; Jansà 1986 1987).

360 The number of WoS meteotsunami papers per year increased from 0 to 2 in the late
361 1980s and early 1990s to more than 2 per year after the mid-2000s (except 2013, Fig. 4b).
362 Interestingly, the peak of the papers was largely connected to special issues of several
363 journals: (i) Physics and Chemistry of the Earth in 2009 (Rabinovich et al. 2009) included 8
364 meteotsunami papers, and (ii) Pure and Applied Geophysics in 2018 (Vilibić et al. 2018a)
365 included 5 meteotsunami papers, while (iii) the third special issue on meteotsunamis, in
366 journal Natural Hazards in 2014 (Vilibić et al. 2014b), was driven by an US project and
367 therefore containing just one paper covering Mediterranean and Black Sea meteotsunamis.
368 While the first special issue in 2009 was dedicated to only meteotsunami research, the second
369 in 2018 covered a variety of Mediterranean and Black Sea meteorology and climatology topics,
370 including meteotsunamis. In total, 10 papers were published between 1990 and 1999, 20
371 between 2000 and 2009 and 24 between 2010 and 2019. Most of these papers have been
372 geographically limited to the Balearic (22) and Adriatic (21) regions (Fig. 5a), while other

373 meteotsunami hot spots (e.g., Strait of Sicily and Maltese Islands) have been only sporadically
374 researched. In addition, 5 papers covered more than one Mediterranean and Black Sea sub-
375 basin or even the whole Mediterranean and/or Black Sea and include research on
376 meteotsunami teleconnections, multi-meteotsunami events or an analysis of high-frequency
377 sea level data. Additionally, all but one paper published prior to 2000 focused on Balearic
378 meteotsunamis, while 11 of the 24 papers between 2000 and 2019 document Adriatic
379 meteotsunamis and the 13 remaining papers cover all regions known for meteotsunami
380 occurrence.

381 Approximately half of the meteotsunami research papers in the Mediterranean and
382 Black Seas are exclusively based on oceanic and atmospheric observations; 10 papers only rely
383 on numerical models, while another 10 papers combine observations and numerical
384 investigations (Fig. 5b). The use of numerical models in Mediterranean and Black Sea
385 meteotsunami research started in 1999, while half of the meteotsunami articles published
386 between 2010 and 2019 included numerical modelling. Eight standalone or combined
387 observation and numerical experiment papers contain analytical solutions used to
388 theoretically derive various meteotsunami processes, particularly for the Balearic Islands.
389 Most of papers investigated both atmospheric and oceanic aspects of meteotsunamis (Fig.
390 5c), with oceanographic studies more concentrated in the Balearic region in which several
391 observational campaigns have been carried out (e.g., LAST-97 experiment, Monserrat et al.
392 1998; Liu et al. 2002).

393

394 **4. Meteotsunami properties**

395

396 *4.1. The source processes and meteotsunamigenic disturbances*

397

398 Several aspects related to the source of meteotsunamis are presented: (i) the
399 resemblance of synoptic patterns related to meteotsunami occurrences and high-frequency
400 sea level oscillations in general, (ii) the mesoscale processes responsible for generation and
401 maintenance of meteotsunamigenic disturbances, and (iii) the manifestation of atmospheric
402 disturbances as high-frequency air pressure or wind oscillations.

403

404 **4.1.1. Synoptic patterns connected to meteotsunamis**

405

406 Atmospheric gravity waves, probably the most frequent source of meteotsunamigenic
407 disturbances, are generated by intense mesoscale processes (such as jets, fronts, convection)
408 related to specific synoptic conditions (Plougonven and Zhang 2014). The relationship
409 between specific synoptic conditions and Balearic meteotsunamis was established in the early
410 1980s (Ramis and Jansà 1983) and has been confirmed in subsequent studies that were mostly
411 focused on specific meteotsunami events (Tintoré et al. 1988; Monserrat et al. 1991a 1991b;
412 Jansà et al. 2007). Šepić et al. (2009a) further analysed this relation and documented that 23
413 out of 32 meteotsunamis (i.e., 72%) in Ciutadella (Balearic Islands) were associated with
414 specific synoptic conditions including: (i) inflow of warm and dry air masses from North Africa
415 at low levels of approximately 850 hPa, (ii) strong winds in the mid-troposphere, higher than
416 20 m/s between 3 and 8 km, and (iii) an unstable layer in the mid-troposphere with a
417 Richardson number lower than 0.25. They found that the correspondence between synoptic
418 conditions and meteotsunami events increased to 88% for the strongest meteotsunamis. The
419 connection between Ciutadella meteotsunamis and specific meteotsunamigenic synoptic
420 patterns has been formally quantified by Šepić et al. (2016a), who constructed a synoptic
421 atmospheric index that increases as the synoptic conditions better match the ideal suggested
422 framework. This research has shown that there exists a threshold below which intense
423 meteotsunami never occur. Still, favourable synoptic conditions for meteotsunamis (high
424 index) are necessary but insufficient, as the exceedance of the threshold is associated with
425 only a 20% probability for meteotsunamis.

426 The connection between synoptic patterns and meteotsunamis in the Balearic Islands
427 preceded the research on Adriatic meteotsunamis, which – aside from early papers – was
428 initiated in mid-2000s and was systematically established for Adriatic events occurring in the
429 2000s and 2010s. The first indication of a similar link between meteotsunamis and synoptic
430 patterns in the Adriatic Sea was derived from the analysis of extreme Bakar Bay seiches (Šepić
431 et al. 2008), which revealed that extreme events are associated with strong south-westerly
432 flow at 700 hPa. Later, several studies documented conducive synoptic conditions observed
433 during the meteotsunami events occurring on 22 August 2007 in Ist, on 15 August 2008 in Mali
434 Lošinj and, retrospectively, on 21 June 1978 in Vela Luka (Belušić and Strelec Mahović 2009;
435 Vilibić and Šepić 2009). However, the middle Adriatic meteotsunami of 27 June 2003 was an
436 exception for which the west-north-western flow was present in most of the atmosphere

437 (Belušić et al. 2007). Systematic investigations of the northern Adriatic meteotsunamis (Šepić
438 et al. 2012) mapped the following favourable synoptic conditions for 16 meteotsunami events
439 observed at the Rovinj tide gauge between 1955 and 2010: (i) a cyclone associated with an
440 approximately 10 hPa drop of air pressure in its centre compared to the climatological mean
441 and stretching north-west from the affected area; (ii) a sharp thermal front at 850 hPa
442 stretching from Algiers over Corsica to the northern Adriatic in the WSW-ENE direction and
443 associated with temperature anomalies of up to 5°C and -4°C southeast and northwest from
444 the front, respectively; and (iii) an anomalously strong mid-troposphere jet at 500 hPa with up
445 to 15 m/s higher velocities than climatological means in the northern Adriatic and northern
446 Italy, just over the affected area and WSW from it.

447 Links to synoptic conditions exist in other parts of the Mediterranean. For example,
448 the events of 27 June 2014 in Odessa (Šepić et al. 2018b) and of 25 June 2014 in Sicily (Šepić
449 et al. 2018a) were studied; these events occurred, along with the Adriatic multi-events (Šepić
450 et al. 2016b), as a sequence of meteotsunamis that hit the Mediterranean and Black Seas,
451 from the Balearic Islands to the northern Black Sea. A systematic investigation of high-
452 frequency sea level events that were measured at 29 tide gauge stations located mostly in the
453 Western and Central Mediterranean was provided by Šepić et al. (2015c), who documented
454 36 events with strong high-frequency sea level oscillations. The events observed at the
455 Balearic Islands, southern Sardinia, Strait of Sicily and southwestern Greece were mostly
456 linked to the same meteotsunamigenic synoptic patterns as those documented for destructive
457 Adriatic and Balearic meteotsunamis (Fig. 6).

458

459 4.1.2. Meteotsunamigenic mesoscale atmospheric processes

460

461 Although specific synoptic atmospheric patterns are definitely associated with
462 meteotsunami events in the Mediterranean and Black Seas, mesoscale processes are key to
463 the generation and propagation of long-lived meteotsunamigenic disturbances. Monserrat et
464 al. (1991a) and Monserrat and Thorpe (1992), first for the Balearic Islands, observed these
465 disturbances in a set of microbarograph measurements and suggested an initial theoretical
466 background based on the wave-duct theory introduced by Lindzen and Tung (1976). Later,
467 Monserrat and Thorpe (1996) fully applied the theory and found that the observed vertical
468 structures of wind and temperature in the lower atmosphere resemble those that allow

469 theoretical modes to propagate long distances in the lower troposphere without a significant
470 loss of energy. These conditions include an unstable layer in the mid or upper troposphere
471 that overtops stable conditions, which are maintained by a dry and warm air. An important
472 prerequisite for wave ducting over long distances is a quasi-linear increase in the wind speed
473 from the ground to the unstable layer, which is normally placed in the mid-troposphere. This
474 unstable layer acts as a reflecting wall that is able to keep the energy related to the
475 atmospheric disturbance in the lower atmosphere. The theory also establishes the
476 relationship between the wind speed at the reflectance mid-troposphere layer with the
477 propagation speed of the atmospheric disturbances (i.e., existence of a critical level within the
478 unstable layer at which these two speeds should be equal).

479 Similar to synoptic patterns, the mesoscale properties of the Adriatic meteotsunamis
480 were found to be associated with the same physical mechanisms as the Balearic events.
481 Several observational studies reproduced the atmospheric conditions favourable for wave
482 ducting, related to the 2007 Ist meteotsunami (Šepić et al. 2009b) and the 2014 middle
483 Adriatic meteotsunami (Horvath et al. 2018), although the latter has also been associated with
484 another mechanism of maintenance and propagation of atmospheric disturbances: the so-
485 called wave-CISK (Conditional Instability of the Second Kind, Powers and Reed 1993). The
486 wave-CISK is characterized by a coupling between a gravity wave and convection, in which
487 convergence associated with the gravity wave forces moist convection, while convective
488 heating provides the energy for the wave. The wave-CISK has been observed and modelled for
489 the 2003 middle Adriatic meteotsunami (Belušić et al. 2007; Fig. 7), in which the atmospheric
490 disturbance was maintained by an anomalously warm Adriatic Sea over ca. 800 km, after its
491 generation over the Alps.

492 Comprehensive investigations of atmospheric mesoscale source processes have not
493 been carried out for other regions, although they have been sometimes attempted, e.g., for
494 the Sicily meteotsunamis (Candela et al. 1999). Still, the data used in the analyses were not
495 appropriate to properly document the mesoscale characteristics of the source; therefore,
496 surface data were restricted to 6-h resolution from a reanalysis. Conditions for wave ducting
497 have also been documented for Black Sea meteotsunamis (Vilibić et al. 2010; Šepić et al.
498 2018b), without applying atmospheric numerical modelling to quantify the processes. In
499 addition, these mechanisms have been proven only for selected meteotsunami events, which
500 normally occur during summer, while a great range of meteotsunamis – including

501 meteotsunamis that occur during winter – have not been researched at all in the
502 Mediterranean.

503

504 4.1.3. Surface manifestation of meteotsunamigenic disturbances

505

506 The first evidence of a relationship between rapid changes in air pressure and
507 meteotsunami waves was suggested rather early, by Fontserè (1934) and Caloi (1938), who
508 analysed a set of events in the Catalan coast and the Balearic Islands, and the northernmost
509 part of the Adriatic Sea, respectively. The relationship was strongly supported by the
510 identification of abnormal rapid oscillations in atmospheric pressure in the operative chart-
511 type barograms that occurred simultaneously with several significant events in the 1970s and
512 1980s in the Balearic Islands (Ramis and Jansà 1983). The first digital atmospheric pressure
513 data with a high enough temporal resolution to identify the properties of atmospheric
514 pressure were not available until the early 1990s (Monserrat et al. 1991a 1991b); however,
515 these observations were sparse and not capable of documenting the spatial characteristics of
516 the air pressure disturbances. The first study that used a triangle of microbarographs
517 (Monserrat and Thorpe 1992) found that the atmospheric disturbances connected with
518 meteotsunamis behave as nondispersive waves, i.e., have no significant variations in their
519 speed with frequency. These data, together with microbarograph data collected during
520 subsequent experiments, have been used to map the spectral characteristics of the
521 atmospheric disturbances (Garcies et al. 1996; Rabinovich and Monserrat 1996; Monserrat et
522 al. 1998) to force an ocean numerical model (Vilibić et al. 2008) and to document severe
523 meteotsunami events (Jansà et al. 2007).

524 In the Adriatic Sea, the microbarograph network was not initially sensitive enough to
525 measure rapid air pressure oscillations. Therefore, no clear records of short period oscillations
526 were derived from measurements for the 1978 Vela Luka meteotsunami. However, the
527 network provided enough information to estimate the speed and propagation direction of the
528 enveloping longest period atmospheric disturbance and to allow the Proudman resonance to
529 be hypothesised as the mechanism responsible for generating meteotsunami waves (Orlić
530 1980). The synchrony between air pressure and sea level observations has been documented
531 from data collected by the newly installed tide gauge in Split (Vilibić and Mihanović 2003). This
532 study preceded the 2003 middle Adriatic meteotsunami for which several operational

533 microbarographs were available to compute the direction and propagation of air pressure
534 disturbances (Fig. 8), which were later used for numerical modelling of the meteotsunami
535 waves (Vilibić et al. 2004). The shape of the air pressure versus the corresponding energy
536 distribution over frequencies was investigated by Vilibić et al. (2005); the results of this study
537 indicated that higher energies are reached below 2 h for cosine versus box-car disturbances.
538 Subsequently, numerous Adriatic meteotsunami studies mapped air pressure disturbances
539 associated with meteotsunamis, including these coming from a triangle of precise
540 microbarographs installed in the middle Adriatic (Vilibić et al. 2014a). They found that, over a
541 great number of strong high-frequency air pressure observations, the atmospheric
542 disturbances were dispersive and therefore had no potential to generate meteotsunamis.
543 Mapping of the spatial and temporal distribution of the intensity, speed and propagation
544 direction of the meteotsunamigenic atmospheric disturbances has been recently improved by
545 an amateur network of lower accuracy but much higher density observations (Šepić et al.
546 2016b).

547 To prove that the multi-meteotsunami events, which occurred in a number of
548 Mediterranean and Black Sea locations, are related to each other, Šepić et al. (2015a) used
549 intense air pressure oscillations collected by different observing networks, which have
550 become standard in recent decades. For other regions, measurements of high-frequency air
551 pressure observations have also been used to investigate meteotsunamis, such as in the Black
552 Sea (Vilibić et al. 2010; Šepić et al. 2018b), south-western Sicily, the Maltese Islands (Drago
553 2009; Šepić et al. 2018a) and the Gulf of Genoa (Pico et al. 2019).

554

555 *4.2. Generation and amplification of meteotsunami waves*

556

557 4.2.1. Open ocean resonant generation

558

559 Following the concurrent observations of intense air pressure oscillations and
560 meteotsunami waves and acknowledging pioneer theoretical work by Proudman in 1929
561 (Proudman 1929), an open ocean resonant mechanism was early assumed to be responsible
562 for the generation of meteotsunami waves. This assumption was particularly applied to the
563 strong seiche events in the Gulf of Trieste (Caloi 1938), which were possibly generated by
564 Proudman resonance. Such a hypothesis has been further proposed by Orlić (1980) for the

565 1978 Vela Luka meteotsunami, who noted the similarity between the speed of the
566 atmospheric disturbance derived from microbarograph observations (~22 m/s) and the
567 predominant speed of long ocean waves off Vela Luka. However, a further study of this event
568 provided by Orlić et al. (2010) revealed a much higher speed of the atmospheric disturbance
569 (34-36 m/s) as the most efficient method for energy transfer towards the sea.

570 Based on reproduction of the 2014 middle Adriatic meteotsunami, Šepić et al. (2016b)
571 introduced the so-called “Proudman length”, i.e., the percentage of the total length over
572 which a disturbance travelled and for which $0.95 < Fr < 1.05$ is valid, where $Fr = U / (gH)^{1/2}$ is the
573 Froude number, U is the atmospheric disturbance speed, H is the water depth and g is gravity.
574 However, the Proudman length was much shorter than necessary to claim that the Proudman
575 resonance is responsible for open-ocean generation of meteotsunami waves (Fig. 9),
576 indicating that some other mechanism might also be important in complex regions of the open
577 middle Adriatic. Indeed, no flat regions are present off the middle Adriatic, creating favourable
578 conditions for maintaining Fr in the short range in which meteotsunamis are efficiently
579 generated (Williams et al. 2020). However, variable bathymetry may generate scattering and
580 reflection of meteotsunami waves, forming and amplifying wave packages at different
581 frequencies as they approach coastal regions (Garrett 1970; Vennell 2007). Reflection is also
582 responsible for the few hours lagged occurrence of meteotsunami waves at the Italian
583 coastline during the 1978 Vela Luka meteotsunami, as these waves travelled back over the
584 Adriatic after impacting the eastern coastline (Orlić et al. 2010).

585 Still, the Proudman resonance has been documented as the major meteotsunami
586 generating force in the relatively flat northern Adriatic (Šepić et al. 2015b) and coastal middle
587 Adriatic waters (Vilibić et al. 2004). Furthermore, Šepić et al. (2015b) note that a small change
588 in the disturbance speed of ca. 10%, which reflects a change in Fr of 10%, may change the
589 open ocean resonance by two or more times. Convincingly, topographic effects play a
590 substantial role even in relatively flat environments, as even a gentle slope was found to
591 substantially decrease the amplification of meteotsunami waves (Williams et al. 2020).

592 For Ciutadella and the Balearic Islands, the idea of resonance was first suggested by
593 Ramis and Jansà (1983), although atmospheric forcing was assumed to resonantly excite the
594 harbour normal modes directly (so-called Chrystal resonance, Bubalo et al. 2018). The first
595 comprehensive theoretical study on processes responsible for generating meteotsunami
596 waves in the Balearic Islands was carried out by Tintoré et al. (1988), who developed an

597 analytical model and suggested resonant generation of coastally trapped edge waves by
598 atmospheric gravity waves, peaking in energy at the same frequencies previously found for
599 their resonant amplification inside the harbour. Gomis et al. (1993), using the first
600 simultaneous sea level and atmospheric pressure observations over the region, demonstrated
601 that an external oceanic wave was necessary as an intermediate mechanism between the
602 atmospheric forcing and sea level oscillations inside the harbour, but suggested that no
603 substantial amplification was expected to occur outside the inlet. The need for intermediate
604 open ocean resonant amplification was also suggested by Rabinovich and Monserrat (1998).
605 They proposed the eventual generation of long ocean waves on the shelf, between Mallorca
606 and Menorca Island, through the Proudman resonance, following the analysis provided for
607 Japanese meteotsunamis (Hibiya and Kajiura 1982). The importance of the Proudman
608 resonance occurring over the shelf off Menorca was later quantified with a numerical model
609 (Vilibić et al. 2008), which found that the resonance definitively plays an initial role in the
610 generation of meteotsunami waves in Ciutadella, although the energy is definitively later
611 amplified by the coastal slope topography and harbour oscillations (Fig. 10). An ocean
612 numerical model forced by synthetic air pressure oscillations was also used by Ličer et al.
613 (2017), who noted that - in any sensitivity scenario - more than 75% of the meteotsunami
614 wave heights reproduced in Ciutadella are formed on the shelf between Mallorca and
615 Menorca, and not on other parts of the shelf.

616 The study by Candela et al. (1999) used observations and simplified barotropic
617 momentum and continuity equations to numerically quantify the ocean gravity modes that
618 are coherently occurring in the Strait of Sicily, which they hypothesize are responsible for
619 generating the southwestern Sicily meteotsunamis. They also emphasize the relevance of the
620 propagating air pressure versus wind disturbances, the latter of which is an order of
621 magnitude lower than the former. The high-precision air pressure and sea level measurements
622 conducted in 2007 and an assessment of bathymetry off the most affected city, Mazara del
623 Vallo, revealed the possible existence of Proudman resonance, associated with edge waves
624 that might occur around the circular outer shelf at the observed frequencies (Zemunik et al.
625 2020). The role of wind disturbances in generating meteotsunami waves has also been
626 quantified by Vilibić et al. (2005), who found their contribution was not more than 30% in the
627 middle Adriatic, where the speed of long ocean waves is between 20 and 30 m/s. However,
628 for shallow regions, such as the coastal northern Adriatic, wind disturbances might be more

629 important, as has been found for other shallow parts of the world ocean (e.g., de Jong and
630 Battjes 2004; Šepić and Rabinovich 2014). The coastal barotropic ocean model forced by
631 measured high-frequency air pressure disturbances travelling with the speed and direction of
632 the wind at 500-hPa reproduced the most observed high-frequency sea level oscillations but
633 also created several false events (Vilibić and Beg Paklar 2006). Air pressure disturbances also
634 have been found to be relevant in the generation of the 2014 Odessa meteotsunami, yet
635 occurred far from the source and were amplified by the Black Sea shelf break almost 200 km
636 off the affected beach. Indeed, for all Mediterranean meteotsunami events that occurred
637 between 23 and 27 June 2014, Šepić et al. (2015a) indicated that suitable resonance
638 conditions (i.e., Fr between 0.9 and 1.1) were present off the affected coastlines, indicating
639 the existence of conditions favourable for occurrence of the Proudman resonance during all
640 these events.

641 In summary, despite several initial investigations that suggest a direct atmospheric
642 forcing on the inlets in several regions, some open ocean resonance amplification of the
643 atmospheric forcing that acts as an intermediate mechanism is necessary to explain the
644 phenomenon. Several processes have been suggested, of which the Proudman resonance is
645 the more plausible open ocean resonant amplification in most of the meteotsunami hot spots.

646

647 4.2.2. Coastal amplification and topographical effects

648

649 Once generated, meteotsunami waves propagate towards the coastline and strongly
650 interact with coastal bathymetry. In fact, the coastal amplification of meteotsunami waves
651 was the first process investigated by researchers, regardless of the open ocean generation
652 mechanism (Airy 1878; Fontserè 1934; Colucci and Michelato 1976; Hodžić 1979/1980; Orlić
653 1980; Ramis and Jansà 1983; Jansà 1986). The theory of seiches and harbour oscillations,
654 worldwide and in the Mediterranean, dates back more than a century (Sterneck 1914; Wilson
655 1972), including the effects of harbour shape on amplification factors (Miles and Munk 1961;
656 Rabinovich 2009). In addition, the exact mechanism of amplification was established rather
657 early. A proper quantification of the amplification was carried out by implementing numerical
658 models, which estimated the quality factor Q for some hot spots, such as Ciutadella ($Q \approx 10$,
659 Rabinovich et al. 1999), Vela Luka ($Q \approx 28$, Denamiel et al. 2018) and other locations.
660 Interestingly, the quality factor may substantially change with interventions that change the

661 inlet geometry, even when these interventions are restricted to the inner parts of the bay. For
662 example, dredging or building new piers and marinas may substantially change the quality
663 factor (Denamiel et al. 2018). There are a great number of studies that have investigated
664 different aspects of harbour resonance during Mediterranean meteotsunamis (Gomis et al.
665 1993; Garcies et al. 1996; Rabinovich and Monserrat 1996 1998; Vilibić and Mihanović 2003;
666 Vilibić et al. 2004; Drago 2008 2009; Orfila et al. 2011), emphasizing the role of resonance in
667 creating extreme sea level oscillations at harbour heads.

668 Harbour resonance may also be modulated by second order effects that may influence
669 the way energy is amplified inside the harbour. For example, the Balearic Islands hot spot –
670 the Ciutadella inlet - is topographically associated with the similar but smaller Platja Gran inlet,
671 forming what would resemble a set of two pendula joined by a string. Liu et al. (2003)
672 documented their resonant coupling through observations and a simple analytical model and
673 found that the coupling is proportional to the distance between the inlets. Further research
674 by Marcos et al. (2004) indicated that these coupling effects may change the amplification
675 factors of each inlet. While such a system was found to slightly decrease oscillations in
676 Ciutadella Harbour, it was found to increase oscillations in Platja Gran.

677 The inclusion of flooding (and drying) of coastal regions into ocean numerical models
678 also has been found to modulate meteotsunami wave heights. This approach is standard in
679 tsunami run-up numerical modelling estimates (e.g., Titov and Synolakis 1998), but not in
680 meteotsunami research. Using the ADCIRC unstructured model, Bubalo et al. (2019) found
681 that the maximum wave height increased 35% at the top of Vela Luka Bay in comparison with
682 the model simulations in which no coastal flooding was included. This might be quite relevant
683 for assessing the associated risk when the meteotsunami waves are several metres high and
684 there is substantial drying or flooding of the coastal region, such as was witnessed during the
685 1978 Vela Luka meteotsunami.

686 A quite unique phenomenon has been observed in the Mazaro River on the southwest
687 coast of Sicily, where a bore propagating upstream has been observed during extreme
688 meteotsunami events (Colucci and Michelato 1976; Candela et al. 1999). It appears that the
689 bore was driven by incoming meteotsunami waves which, due to the shallow and narrowing
690 waterway and its relatively wide V-shaped mouth, met conditions that enabled the bore to
691 form a half kilometre upstream of the mouth (Šepić et al. 2018a, Fig. 11). There, the bore may
692 rise to a metre or more and propagate upstream a few kilometres, damaging small and fishing

693 boats along its way. It should be emphasized that the incoming open ocean waves are
694 additionally amplified by the Mazara del Vallo harbour, before entering the river at the top of
695 the harbour.

696 In addition to harbour resonance, meteotsunami waves have been found to be
697 affected by coastal topography in different ways. Off the southwestern Sicily, a few kilometres
698 wide channel that separates the inner (coastal) and outer (open sea) shelf may affect the
699 meteotsunami waves that arrive at Mazara del Vallo (Šepić et al. 2018a). Off Ciutadella, a
700 shoaling affects the amplification of the incoming meteotsunami waves, by more than 4 times
701 over just a few kilometres (Vilibić et al. 2008; Fig. 12). Similar amplifications occur in other
702 coastal regions off meteotsunami hot spots (e.g., Vela Luka, Orlić et al. 2010; Šepić et al.
703 2016b), yet these effects have not been quantified by numerical modelling exercises. When
704 meteotsunami waves last for several hours and occur over hundreds of kilometres, as
705 occurred during the Odessa 2014 meteotsunami, the waves may be channelized by
706 underwater canyons and propagate as rays towards the exact beaches impacted by waves
707 (Šepić et al. 2018b). Such propagation characteristics further resembles the similarities
708 between propagation of meteotsunami and tsunami waves, which are known to be directed
709 by underwater ridges and canyons (Okal and Synolakis 2008; Iglesias et al. 2014).

710 A better knowledge of the role of coastal amplification of meteotsunami may be
711 obtained by separating the effects of the forcing mechanism from those of the coastal
712 amplification in the energy spectra observed at coastal locations. A pioneering study was
713 carried out by Monserrat et al. (1998), who modified the existing algorithm to separate the
714 source and topography previously used for seismic tsunamis by Rabinovich (1997). For a given
715 event, those similarities observed at different but nearby locations should be related to the
716 forcing and differences due to the coastal amplification. However, for different events
717 measured at a given location, similarities should be related to the coastal amplification at this
718 point and differences in the forcing. When they computed the spectral ratios
719 (event/background) measured at different locations during the same event, the effect of the
720 coastal amplification was removed and the ratios became very similar, elucidating the forcing
721 characteristics for this event (Fig. 13). They also showed that by computing the forcing
722 characteristics of different events and dividing by the observed atmospheric energy during
723 each event, the energy contents should show how the atmospheric energy is transferred to
724 the ocean. These spectral contents were very similar, suggesting that the atmospheric energy

725 during different meteotsunami events was transferred into the ocean in a similar manner (Fig.
726 13c). These similarities have been used to analyse oscillations at Ciutadella and Cala Ratjada
727 (Menorca Island) where oscillations normally occur first, indicating that sea level
728 measurements at Cala Ratjada could be used to forecast destructive events in Ciutadella
729 (Marcos et al. 2009).

730

731 *4.3. Teleconnections between different regions in the Mediterranean*

732

733 Meteotsunamis are normally local phenomena, associated with several specific
734 mesoscale features that rapidly change in time and space, affecting a few nearby locations.
735 However, these mesoscale features are always linked to several specific atmospheric synoptic
736 pattern which may affect large regions and/or last long enough to travel large distances. This
737 implies that meteotsunami events may be simultaneously observed in different sites located
738 relatively far away as the synoptic situation favourable to their generation affect a large area
739 or if the synoptic pattern evolves and travels long distances.

740 These teleconnections between meteotsunamis observed in distant regions were first
741 suggested by Šepić et al. (2009a) for the Mediterranean Sea. By analysing a set of 32 events
742 reported in the Balearic Islands for the period 1975-1998, the authors found that a significant
743 number (approximately 50%) were also observed, in a 48-h time window, in the Adriatic Sea.
744 When concurrent or subsequent meteotsunamis were observed in both regions, the events
745 were always associated with a specific synoptic pattern, which either simultaneously affected
746 both areas or propagated from one region to the other.

747 These teleconnections became even more apparent after analysing the 23-27 June
748 2014 meteotsunamis, during which an atmospheric synoptic pattern propagated eastward
749 over the Mediterranean and generated a chain of destructive meteotsunami events that
750 affected several countries from Spain to Ukraine (Fig. 14, Šepić et al. 2015a). The synoptic
751 conditions favourable to the generation of meteotsunamis, as described in the previous
752 section, were first observed over the Balearic Islands on 23 June, then propagated to the east,
753 over the Adriatic and Tyrrhenian seas (25-26 June) and finally reached the Black Sea on 27
754 June. The greatest sea level oscillations were observed in each region at the time of the most
755 intense atmospheric instability and when a completely developed mid-troposphere jet stream
756 was located over the given area.

757 This reported chain of events revealed that meteotsunamis should not be only
758 considered as local phenomena but as a potentially dangerous regional risk that can affect
759 large areas, within distances of thousands of kilometres.

760

761 **5. Meteotsunami monitoring and forecasting systems**

762

763 Meteotsunami detection systems rely on four different components used either
764 separately or in combination (Vilibić et al. 2016): (i) identification of tsunamigenic atmospheric
765 synoptic conditions, (ii) real-time high-frequency air pressure and sea level measurements,
766 (iii) high-resolution atmospheric and ocean deterministic forecast, and (iv) stochastic
767 meteotsunami hazard assessments. Due to their cost, these systems are evolving with the
768 available technology and are still underdeveloped in the Mediterranean Sea where the
769 meteotsunami hazard is often overlooked by coastal managers. In fact, at this time, only two
770 research products have been fully tested and published: the Balearic Rissaga Forecasting
771 System (BRIFS; Renault et al. 2011) and the Adriatic Sea and Coast (AdriSC) system (Denamiel
772 et al. 2019a 2019b) (Fig. 15).

773

774 *5.1. Observational networks*

775

776 In the Balearic Islands, 1-min real-time sea level and air pressure records are available
777 at 6 tide gauge locations (Andratx, Colonia de Sant Pere, Pollensa, Porto Cristo, Sa Rapita and
778 Sant Antoni) and 20 air pressure sensor locations operated by SOCIB (Balearic Islands Coastal
779 Observing and Forecasting system) and are displayed at
780 <http://www.socib.es/index.php?seccion=observingFacilities&facility=mooring> (Fig. 15, Tintoré et al.
781 2013, Heslop et al. 2019). Based on these Balearic tide gauge measurements, a detection
782 algorithm analysing intermittent sea level oscillations and identifying meteotsunami events -
783 via wavelet analysis and more precisely averaged power spectral densities - was developed by
784 André et al. (2013).

785 In the Adriatic Sea, a pilot microbarograph network of three air pressure sensors with
786 a sampling rate of 1 min, used for real-time detection of intense air pressure disturbances,
787 was first developed by Šepić and Vilibić (2011). Within this system, the air pressure rate of
788 change is determined every 5-min and, when a meteotsunamigenic disturbance is identified,

789 its intensity, period, speed and direction of propagation are automatically calculated. Similar
790 to the procedure developed by Tinti et al. (2012) for seismic tsunamis, the parameters
791 measured are then compared with the meteotsunami warning matrix estimated from
792 historical events. The Adriatic microbarograph network was extended in 2017 to the whole
793 middle Adriatic region by the MESSI project (“Meteotsunamis, destructive long ocean waves
794 in the tsunami frequency band: from observations and simulations towards a warning
795 system”, <http://www.izor.hr/messi>). Presently, the network encompasses nine air pressure
796 sensors located in (1) the eastern Adriatic meteotsunami hot spots of Vela Luka, Stari Grad,
797 and Vrboska, (2) the middle Adriatic islands of Vis, Svetac and Palagruža, to quantify the spatial
798 changes in atmospheric disturbances over the regions in which resonance is expected to
799 occur, and (3) Ancona, Ortona, and Vieste, located on the Italian coast, providing the
800 parameters needed for the early warning system at coastlines where the atmospheric
801 disturbance is expected to occur over the Adriatic Sea. The network also includes three tide
802 gauges located in Vela Luka, Stari Grad and Sobra (Fig. 15). In addition to being used for
803 meteotsunami detection, these measurements are also invaluable for the evaluation of the
804 modelling tools used in the Adriatic Sea (Denamiel et al. 2019a 2019b).

805 In addition, the meteotsunami community has been collaterally benefiting from large
806 investments made in a real-time 1-min sea level worldwide network developed for tsunami
807 research and managed by the Intergovernmental Oceanographic Commission (IOC,
808 <http://www.ioc-sealevelmonitoring.org/map.php>). In the Mediterranean and Black Seas, this
809 network encompasses more than 120 stations operational in real-time or near-real-time,
810 principally used to support verification of new tsunami forecasts (Angove et al. 2019);
811 however, this network still has an insufficient spatial coverage to properly identify
812 meteotsunamis with scales of a few tens of kilometres or less (Vilibić et al. 2016).

813

814 *5.2. Deterministic modelling tools*

815

816 Both meteotsunami detection systems developed in the Mediterranean Sea are based
817 on the same state-of-the-art numerical models: the Weather Research and Forecasting model
818 (WRF, Skamarock et al. 2005) for the atmosphere and the Regional Ocean Modelling System
819 (ROMS, Shchepetkin and McWilliams 2005 2009) for the ocean, although the modelling
820 strategy implemented in each is quite different.

821 In BRIFS (Renault et al. 2011), the WRF and ROMS models are coupled off-line, which
822 means that the two grids of the WRF model, which cover the Western Mediterranean basin
823 with a resolution of 20-km and the area around the Balearic Islands with a 4-km resolution,
824 are run for a 12-h spin-up and 24-h forecast period (as described in Fig. 15). Then, the 2-min
825 sea level pressure is extracted from the WRF 4-km results and used to force the two ROMS
826 grids for the 24-h forecast period, covering the Balearic Islands with a resolution of 1 km and
827 the Ciutadella harbour with a resolution of 10 m. The WRF model is set up with 97 vertical
828 levels, refined near the surface to properly resolve the inversion layer associated with *rissaga*,
829 and initialized/forced at the boundaries with the FNL/GFS analysis/forecast from the National
830 Centers for Environmental Prediction (NCEP). The ROMS model, however, is not forced by any
831 density stratification at the boundaries.

832 In the AdriSC system (Denamiel et al. 2019a), the WRF and ROMS models are coupled
833 on-line every minute within the Coupled Ocean-Atmosphere-Wave-Sediment-Transport
834 (COAWST) modelling system developed by Warner et al. (2010). The WRF domains over the
835 central Mediterranean basin have a resolution of 15 km while those over the entire Adriatic
836 and Ionian Seas have a 3 km resolution. The ROMS domains also cover the Adriatic and Ionian
837 Sea with a 3 km resolution and the Adriatic Sea with a 1 km resolution. Terrain-following
838 coordinates are used for vertical discretization in both ocean and atmosphere models,
839 containing 58 vertical levels in WRF refined in the surface layer (Laprise 1992) and 35 vertical
840 levels in ROMS refined near both the sea surface and bottom floor for the ocean (Shchepetkin
841 and McWilliams 2009). The initial state and boundary conditions are taken from the European
842 Centre for Medium-Range Weather Forecasts (ECMWF) Atmospheric Model high resolution
843 10-day forecast (HRES – Lalaurette 2002; Petroliağis and Pinson 2012; Zsótér 2006; Zsótér et
844 al. 2014) and the Mediterranean Forecasting System (MFS) high resolution 10-day MEDSEA
845 forecast (Pinardi et al. 2003; Pinardi and Coppini 2010; Tonani et al. 2014).

846 In addition to the COAWST model which is run for a 48-h spin-up and 24-h forecast
847 period, an even more refined WRF domain covering the Adriatic Sea with a 1.5-km resolution
848 is coupled off-line with the unstructured ADvanced CIRculation ocean model (ADCIRC,
849 Luettich et al. 1991) for a 12-h spin-up and 24-h forecast period covering the last 36-h of the
850 COAWST model run (as described in Fig. 15). The ADCIRC mesh is specifically designed to
851 provide extreme sea level hazard assessments in Croatia, covering the entire Adriatic Sea with
852 a minimum resolution of 100 m along the Croatian coastline and up to 10 m in the harbours

853 of interest (e.g., Vela Luka, Stari Grad, Vrboska, etc.). The ADCIRC model is forced with 1-min
854 high-resolution air pressure and wind stress.

855 In terms of modelling strategy inter-comparison, BRIFS, which is less computationally
856 expensive, is most probably faster but only provides next day forecasts with atmospheric
857 forcing at a 4-km resolution. This resolution is known to be too coarse to properly represent
858 meteotsunamigenic disturbances in the Mediterranean Sea (Horvath et al. 2018). The AdriSC
859 system can be used to detect air pressure disturbances at 1.5-km resolution at least 30-h in
860 advance. In addition, as the WRF wind fields are also used to force the ocean models (ROMS
861 and ADCIRC), the AdriSC system, which includes a wave component, can forecast
862 atmospherically driven extreme sea level events other than meteotsunamis. However, due to
863 the lack of computational resources and the numerical cost of the modelling suite, the AdriSC
864 system is currently not operational, while BRIFS has run without interruption over the last
865 decade in the Balearic Islands.

866

867 *5.3. Stochastic hazard assessment*

868

869 Due to the challenges posed by deterministic forecasting of the meteotsunamigenic
870 atmospheric disturbances in the Mediterranean Sea, it is of prime importance to assess how
871 sensitive meteotsunami hazards are to their direction, intensity, period and speed at hot spot
872 locations. In the Balearic Islands, several sensitivity studies have assessed the meteotsunami
873 hazards in Ciutadella (Marcos et al. 2003; Vilibić et al. 2008; Orfila et al. 2011) for individual
874 events. Ličer et al. (2017) generalized this approach and used 160 numerically generated
875 synthetic atmospheric gravity waves to stochastically investigate the meteotsunami
876 amplification and propagation inside and outside Ciutadella harbour. The study followed
877 previously documented conclusions and found that, given the shape of the Balearic
878 bathymetry, a wide range of gravity wave speeds (between 23 and 36 m/s) and angles of
879 propagation (between 210° and 250°) can lead to substantial meteotsunami amplification (Fig.
880 16). Furthermore, they found that amplification mainly occurs in the Menorca Channel
881 (described as a focusing lens). The findings of this study thus demonstrate the difficulty in
882 providing timely meteotsunami warning in Ciutadella when the pressure disturbances are
883 locally generated in the Menorca Channel.

884 In the Adriatic Sea, a similar approach was used by Orlić et al. (2010) and Šepić et al.
885 (2016b), who based sensitivity studies on simplified synthetic disturbances following
886 observations from the 1978 Vela Luka and the 2014 middle Adriatic meteotsunamis,
887 respectively. They found a disturbance speed of 28-36 m/s, which depended on the
888 meteotsunami hot spot affected, i.e., Vela Luka Bay, Stari Grad Bay and Rijeka dubrovačka
889 Bay, and the propagation direction of the disturbance. For the latter, the disturbances that
890 generate the maximum meteotsunami waves were found to travel from 200-240°, 260-300°
891 and 260-290° for Vela Luka, Stari Grad and Rijeka dubrovačka, respectively. For the northern
892 Adriatic meteotsunami sites at Široka Bay (Ist Island) and Mali Lošinj Bay, the greatest
893 resonant transfer of energy towards the sea is reached at smaller propagation velocities due
894 to the decreasing ocean depth encountered towards the northwest (Šepić et al. 2015b). As
895 the ocean is quasi-flat in the northern Adriatic, this sensitivity study suggests that the
896 Proudman resonance is the dominant resonance mechanism in that location.

897 With the same approach, Šepić et al. (2018b) showed that the most efficient
898 generation of meteotsunami waves during the 2014 Odessa meteotsunami occurred on the
899 shelf break, where the disturbance travelled in parallel to the shelf break, while the
900 meteotsunami waves generated were topographically directed towards the north and the
901 affected beaches.

902 Denamiel et al. (2018) improved the methodology and assessed the impact of
903 geomorphological changes (i.e., deepening of the bay, dredging the harbour, removing an
904 island, adding a pier or a marina) to the Vela Luka harbour resonance during all potential
905 meteotsunami events. The meteotsunami impacts were assessed for a set of 6401 synthetic
906 air pressure fields used to derive robust statistics. In contradiction to the values obtained with
907 the traditional quality factor derived from the peak frequency of the sea level spectrum, the
908 most substantial increase in meteotsunami amplification was obtained when the Vela Luka
909 harbour was dredged to 5 m depth. New values of the quality and amplification factors were
910 thus re-calculated by integrating the forcing energy content over the full frequency range and
911 were found to be in good agreement with the results of the statistical analysis in Vela Luka
912 Bay (Fig. 17).

913 Finally, in the Adriatic Sea, a meteotsunami surrogate model based on the generalized
914 Polynomial Chaos Expansion (gPCE; Soize and Ghanem 2004; Xiu and Karniadakis 2002) was
915 developed by Denamiel et al. (2019b 2020). The model uses polynomial expansions to project

916 the probability distribution of the maximum meteotsunami elevation and estimates the
917 meteotsunami maximum elevation distributions at meteotsunami hot spots by propagating
918 the uncertainty in the atmospheric forcing to ocean simulations. With this approach, the
919 sensitivity to the atmospheric disturbance parameters (start location, direction, speed, period,
920 amplitude, and width of the disturbance) may be quantified. The surrogate model, which can
921 use either deterministic forecast results or measurements from air pressure sensors as input
922 parameters, is designed to assess the potential hazard of any meteotsunami event in the
923 middle Adriatic region in only a few minutes (practically at no computational cost) and for a
924 large number of samples. In addition, the gPCE formulation allows for the analytical
925 computation of Sobol' indices (Sobol' 2001; Saltelli et al. 2008; Sudret 2008) used to
926 systematically derive, in the Adriatic Sea, the meteotsunami sensitivity to the six chosen
927 stochastic parameters of the atmospheric disturbance without any additional computations.
928 Not surprisingly, this sensitivity analysis revealed that, for all hot spot locations in the Adriatic
929 Sea, the speed or the period of the atmospheric disturbance is the most critical parameter for
930 meteotsunami harbour amplification, while the effects of the amplitude are of secondary
931 importance.

932 While stochastic approaches have only been recently successfully implemented in the
933 Balearic and Adriatic regions, they certainly provide important insights concerning
934 meteotsunami amplification linked to atmospheric forcing. This approach must be further
935 developed in both theoretical and operational studies to compensate for the lack of accuracy
936 in the deterministic atmospheric models and to better quantify the uncertainty associated
937 with meteotsunami forecasting.

938

939 *5.4. Meteotsunami early warning systems*

940

941 As fully preventing meteotsunami impacts is, for now, close to impossible (Vilibić et al.
942 2016), the principal goal of meteotsunami early warning systems is to enable the local
943 communities to better prepare for these destructive events (e.g., set up temporary
944 protections against flooding and waves, avoid swimming, etc.) to minimize losses. Such a
945 warning system can be based on different observational and modelling tools: (i)
946 meteotsunamigenic synoptic patterns, (ii) in situ high-frequency observations, and (iii)
947 deterministic and/or stochastic numerical modelling, or a combination of these (Šepić et al.

948 2017). For the Balearic Islands, the “rissaga warning” is operational up to two days before
949 potential meteotsunamis; however, it is based on qualitative (by a human eye) assessment of
950 forecasted operational synoptic patterns (Jansà et al. 2007). The warning system has been
951 found to fairly forecast moderate meteotsunami events (75-150 cm of wave height in
952 Ciutadella), with a correct forecast in approximately 75% of such events between 2003 and
953 2006 (Jansà and Ramis 2020). Still, the strongest meteotsunamis (>150 cm of wave height in
954 Ciutadella) are mostly underestimated (in 85% of cases), indicating the existence of specific
955 atmospheric conditions not attainable from synoptic patterns.

956 The quantification of the connections between synoptic patterns and multi-year sea
957 level observations was also improved by Šepić et al. (2016a) with the definition of the so-called
958 synoptic meteotsunami index (Section 4.1.1), which can also be used to assess meteotsunami
959 changes in the future climate. The latter has been conducted by Vilibić et al. (2018b), who
960 found that meteotsunami occurrences will increase by 1/3 in Ciutadella for the RCP8.5
961 scenario during the 2071-2100 period. Until now, no such operative tool was developed in
962 other Mediterranean basins - e.g., the Adriatic Sea - although favourable meteotsunamigenic
963 synoptic conditions have been documented. In addition, despite the known propagation of
964 meteotsunamigenic synoptic patterns from the Western to the Eastern Mediterranean and
965 the Black Sea, a large scale meteotsunami early warning based on synoptic conditions has not
966 been developed.

967 Romero et al. (2019) modified the modelling approach in an meteotsunami early
968 warning system to reproduce key atmospheric and ocean processes, such as (i) the generation
969 of high amplitude atmospheric gravity waves upstream from the Balearic Islands and travelling
970 in the SW–NE direction; (ii) the oceanic response to the respective pressure fluctuations along
971 the Menorca channel; (iii) shelf amplification, which doubles the wave amplitude; and (iv) the
972 harbour resonance within Ciutadella inlet. They tested the simplified warning system on 126
973 meteotsunamis between 1981 and 2018 and found the best performance for weak
974 meteotsunamis (<20 cm of wave height in Ciutadella), while for intense (100-200 cm of wave
975 height in Ciutadella) and extreme (>200 cm of wave height in Ciutadella) meteotsunamis the
976 proper reproduction (in the same intensity category) was achieved for 43 and 33% of
977 meteotsunamis, respectively.

978 However, an advanced prototype of a meteotsunami early warning system (Fig. 18)
979 was developed and successfully evaluated in the Adriatic Sea (Šepić et al. 2017, Denamiel et

980 al. 2019b), but it is unfortunately not operational due to a lack of computational resources.
981 This early warning system receives two different type of data: high-resolution atmospheric
982 and ocean model results provided by the AdriSC system and 1-min measurements from the
983 MESSI observational network. Both are used as input to the meteotsunami stochastic
984 surrogate model (presented in Section 5.3) to provide extreme sea level hazard assessment at
985 hot spot locations along the Croatian coastline. In the daily operational mode (Fig. 18), the
986 high-pass filtered sea level pressure is automatically extracted from the WRF 1.5-km results at
987 least 24 h before any potential meteotsunami event. If a pressure disturbance is detected, the
988 meteotsunami maximum elevation distributions (i.e., the probability of the expected
989 maximum elevation) are computed at different locations of interest by the stochastic
990 surrogate model. The maximum elevation probability distributions are revised 2 h before the
991 forecasted meteotsunami event, by analysing the 1-min air pressure measurements from
992 Ancona, Ortona, Vieste, Svetac, and Vis, and imposing the extracted disturbance parameters
993 as constant input values in the model. The final meteotsunami warning is then ready to be
994 published and accessible to users. This system was tested on five meteotsunami events that
995 occurred between 2014 and 2018 and yielded a fair forecast but overestimated several
996 episodes (Denamiel et al. 2019b).

997

998 **6. Research gaps and emerging research topics**

999

1000 As presented in this review, meteotsunami research has a long tradition in the
1001 Mediterranean and Black Seas, where extreme events strongly impact shores, cities and
1002 coastal infrastructures. However, in the last decade, it has substantially developed all over the
1003 world due to the net increase in available high-frequency sea level and meteorological
1004 observations. Observational networks have indeed expanded globally (e.g., IOC Sea Level
1005 Station Monitoring Facility network (<http://www.ioc-sealevelmonitoring.org/>) or regionally
1006 (e.g., NOAA Tides and Currents, <https://tidesandcurrents.noaa.gov>), enabling for mapping of
1007 high-frequency sea level oscillations and meteotsunamis in all continents (Rabinovich 2020).
1008 In recent years, a great number of meteotsunami studies have been carried out around the
1009 world based on observations, modelling and analysis of source processes and in relation to
1010 geographical location and local processes (Pellikka et al. 2014; Linares et al. 2016 2019;
1011 Sheremet et al. 2016; Olabarrieta et al. 2017; Dusek et al. 2019; Kim et al. 2019; Williams et

1012 al. 2019; Heidarzadeh et al. 2020; Shi et al. 2019 2020), which can produce meteotsunamis of
1013 different origins than those in the Mediterranean (e.g., frontal zones, hurricanes).

1014 The idea of this chapter is to present research gaps and ideas for future research
1015 considering specific Mediterranean and Black Sea meteotsunami issues, but that are also
1016 relevant to global meteotsunami research in addition to regional considerations. We classified
1017 these ideas into two major categories: (i) improvement of research tools and (ii)
1018 meteotsunami research topics themselves:

1019

1020 ***A. Tools for meteotsunami research***

1021

1022 A.1. Extension of high-frequency sea level observations over the whole basin. To properly
1023 quantify spatial properties of high-frequency oscillations, the extension of available sea level
1024 networks over the entire Mediterranean and Black Sea shores is necessary. Presently, most of
1025 these stations are located along the northern shores of the Mediterranean, while the Black
1026 Sea and the North Africa coastlines are sparsely populated with high-frequency sea level
1027 observations. A unification of such a network (e.g., through a regional Global Ocean Observing
1028 System, MonGOOS, www.mongoos.eu) might be adequate to tackle eventual political or
1029 funding problems that generally prevent such developments.

1030

1031 A.2. Extension of conjoint high-frequency sea level and meteorological observations. The
1032 current standard in meteorological measurements, temporal resolutions of 10 min to 1 h, is
1033 not appropriate for observations of meteotsunamigenic disturbances. Presently, only the
1034 SOCIB and MESSI networks have a potentially appropriate spatial resolution for meteotsunami
1035 research in the Mediterranean region. Efforts to upgrade existing networks (e.g., those
1036 presented in the IOC Sea Level Station Monitoring Facility network) and influence national
1037 meteorological services to distribute data with at least 1-min resolution should be undertaken.
1038 As the technology is mostly ready at actual measuring stations, this should not require large
1039 investments.

1040

1041 A.3. Improvement and better usage of amateur meteorological networks and citizen science.
1042 Aside from official and standardized meteorological observations, many amateur
1043 meteorological networks (e.g., Crometeo in the eastern Adriatic Sea, www.pljusak.com, or

1044 global Wunderground network, <https://www.wunderground.com>, also active in the
1045 Mediterranean and Black Seas, or Balearsmeteo in the Balearic Islands,
1046 <http://balearsmeteo.com>) can be used by the research community. These networks do not
1047 follow all official meteorological standards and might not be properly calibrated, yet they may
1048 provide extremely valuable information on high-frequency air pressure and wind data (e.g.,
1049 Šepić et al. 2016b) with very good spatial resolution. In addition, school meteorological
1050 networks might also be used in research, for example, the School-Based Weather Station
1051 Network on the Vancouver Island (<http://www.islandweather.ca>, Rabinovich et al. 2020).
1052 Thus, extending and improving such networks through a citizen science approach (Garcia-Soto
1053 et al. 2017) would probably help in quantification of spatial and temporal properties of
1054 meteotsunamigenic disturbances.

1055

1056 A.4. Development and installation of state-of-the-art observing platforms adapted to
1057 meteotsunami research. As measuring both meteotsunami waves and meteotsunamigenic
1058 disturbances requires quite different standards than the ones used by the current
1059 observational networks, standards used in new platforms should be adapted to the
1060 meteotsunami research. As an example, high-frequency radars, when used in burst mode (Lipa
1061 et al. 2014), have been found to be useful for detecting meteotsunami waves off the
1062 Mediterranean and Black Sea coastlines (Roarty et al. 2019). At hot spot locations, the
1063 automatic extraction of the speed, propagation direction and intensity of meteotsunamigenic
1064 disturbances can be developed from well calibrated and verified high-frequency weather
1065 radar observations (e.g., following the concept developed for minute weather forecast by
1066 AccuWeather; <https://www.accuweather.com/en/press/49568860>). In addition, the future
1067 advancement in technology may also allow for the development of efficient and cheap
1068 solutions (e.g., Marques et al. 2019), such as self-communicating autonomous networks of
1069 sensors measuring meteorological parameters at high frequencies.

1070

1071 A.5. Availability of precise coastal bathymetry at meteotsunami hot spot locations. As is used
1072 for other ocean processes, proper bathymetry at high resolution is necessary to accurately
1073 reproduce meteotsunamis in numerical studies. This particularly applies to all Mediterranean
1074 and Black Sea hot spots, for which only old charts are available and where a small change in
1075 bathymetry may multiply or reduce the estimated meteotsunami wave heights (e.g., Denamiel

1076 et al. 2018). Thus, meteotsunami hot spots such as Vela Luka, Ciutadella and other locations
1077 should have priority for hydrographic surveys performed with modern mapping technologies
1078 (e.g., lidar, Brock and Purkis 2009).

1079

1080 A.6. Development of ocean models with high-resolution bathymetry. Recent studies show that
1081 processes occurring nearshore, such as rip currents, may be associated with meteotsunamis.
1082 In addition, meteotsunami models still rarely consider coastal flooding effects on the
1083 amplification and run-up of meteotsunami waves. To numerically capture such processes, a
1084 few metres horizontal resolution is necessary (Linares et al. 2019). Similarly, for complex
1085 topography such as in the Mediterranean, models with unstructured grids with down to a
1086 metre resolution in the coastal regions (both in sea and at land) are necessary to properly
1087 quantify the bathymetric effects on the development and amplification of meteotsunami
1088 waves (e.g., Vilibić et al. 2008; Denamiel et al. 2018). For the open sea, the bathymetry should
1089 also be of high enough resolution to reproduce scattering of meteotsunami waves, particularly
1090 in regions with a complex and changeable bathymetry.

1091

1092 A.7. Development of ultra-high-resolution mesoscale atmospheric models reproducing
1093 meteotsunamigenic disturbances and processes. Even with the right set-up, ocean models
1094 may misrepresent meteotsunami waves due to the difficulty in properly reproducing
1095 meteotsunamigenic disturbances within mesoscale atmospheric models. Several bottlenecks
1096 that affect the reliability of mesoscale atmospheric simulations have been identified (e.g.,
1097 Horvath and Vilibić 2014): proper initialisation, reliable lateral boundary conditions, choice of
1098 parameterizations as well as horizontal and vertical resolutions used in the models. As
1099 meteotsunamigenic disturbances occur at a kilometre spatial scale, the horizontal model
1100 resolution needed is a few hundreds of metres, since mesoscale atmospheric models
1101 underestimate processes at scales lower than 7 times the horizontal resolution (Skaramock,
1102 2004). However, the physics of state-of-the-art atmospheric models may not be adaptable to
1103 run at these resolutions. Therefore, new approaches in mesoscale modelling should be
1104 developed, and tested specifically for meteotsunamis, in collaboration with leading
1105 atmospheric model developers (such as National Centres for Atmospheric Research, NCAR).
1106 This issue is foreseen as critical in proper deterministic reproduction of meteotsunamis,
1107 including the application of operational forecasting and early warning systems.

1108

1109 A.8. Availability of high-performance computing (HPC) facilities for ultra-high-resolution
1110 numerical modelling. Following issues raised in A.7, access to HPC facilities is a prerequisite to

1111 carry out such a research. For meteotsunami coupled atmosphere-ocean systems, the three
1112 dimensional atmospheric part requires the most computational resources and including ultra-
1113 high resolutions will increase demand by one to two orders of magnitude.

1114

1115 A.9. Development of stochastic methods in meteotsunami research. As noted above,
1116 deterministic reproduction of meteotsunamis and meteotsunamigenic disturbances are not
1117 reliable enough to be solely used in forecast and early warning systems. The recent attempts
1118 at applying stochastic methods in meteotsunami research are encouraging and have resulted
1119 in better assessments of meteotsunami hazards than the deterministic approaches, while
1120 demanding much less computational resources. Such approaches also allow for quantification
1121 of uncertainties of the meteotsunami forecast, for which deterministic models have no
1122 capacity (except if run as ensemble forecast, which would then be extremely costly in terms
1123 of numerical resources). In general, stochastic methods are not widely used in ocean research
1124 and their applications in meteotsunami research might thus be encouraging for wider hazard
1125 assessments of atmospherically driven extreme sea levels.

1126

1127 A.10. A framework for collaborations, research, operational issues and definition of standards
1128 in meteotsunami research. All the tools listed above could potentially improve meteotsunami

1129 research and would be developed much more efficiently within multidisciplinary
1130 collaborations encompassing research groups with expertise in all quoted issues using
1131 common resources. For example, a WRF model of 15-km resolution may be set-up for the
1132 entire Mediterranean and Black Seas and provide everyday hourly forecast results that could
1133 be downscaled (up to 1-km resolution) directly in hot spot areas. Further, the meteotsunami
1134 community should take advantage of the already developed tsunami infrastructures, which
1135 have teams of operators monitoring seismic activity 24/7 that could be trained to also monitor
1136 meteotsunamis. Such a collaborative effort is a priority to better use the limited resources
1137 allocated to research and to provide services (i.e., meteotsunami warning) to the society. The
1138 Mediterranean and Black Sea meteotsunami collaborations could be part of global formal
1139 collaborations, in addition to being dedicated to the specific issues in the region. The recently

1140 held First World Conference on Meteotsunamis (www.izor.hr/mts2019) established new
1141 collaborations and the enthusiasm should be used to progress in a direction of collaboration.

1142

1143 ***B. Meteotsunami research topics***

1144

1145 B.1. Analysing basin-wide high-frequency sea level events, including their statistics,
1146 climatology and probabilistic recurrence functions. Once gaining multi-year or multi-decadal
1147 high-frequency sea level dataset, i.e., from the IOC Sea Level Station Monitoring Facility portal
1148 or through national networks (e.g., Croatian tide gauges are collecting sea level data with 1-
1149 min resolution since 2003), an objective mapping of meteotsunamis and high-frequency
1150 oscillations might be carried out, such as was documented for the U.S. East Coast (Dusek et al.
1151 2019). This might also include different statistical aspects such as seasonality, outreach,
1152 connection with synoptic patterns, teleconnections, all of which have already been initially
1153 analysed in several studies (e.g., Šepić et al. 2009a; 2015c); additional studies could be based
1154 on more comprehensive datasets and generalized. For several sites with particularly long
1155 measurements, the return periods for meteotsunami events might even be estimated.

1156

1157 B.2. Quantifying relations between meteotsunamis and synoptic patterns. Although the link
1158 between meteotsunamis and synoptic patterns has been documented for several
1159 Mediterranean and Black Sea hot spots, the only study that quantifies these relations is for
1160 the Balearic Islands (Šepić et al. 2016b). Therefore, this approach may be extended to other
1161 hot spots to understand which patterns, if any, are relevant for meteotsunamis at those
1162 locations. If such a mapping provides reliable results at the basin level, this might be used for
1163 proxy-based assessment of meteotsunami characteristics, as atmospheric reanalysis fields
1164 cover longer periods than high-frequency sea level measurements.

1165

1166 B.3. Investigating wintertime Mediterranean and Black Sea meteotsunamis and other source
1167 mechanisms. Most of the investigated Mediterranean and Black Sea meteotsunamis, i.e., the
1168 most destructive events, occurred during warm part of the year, between April and October.
1169 However, moderate meteotsunami events may occur during wintertime and may be related
1170 to generation mechanisms different than those observed in summertime, i.e., to wind
1171 pulsations during storms or other, as high-frequency air pressure disturbance are of lower

1172 intensity in winter (Vilibić et al. 2014a). Furthermore, different generation mechanisms for
1173 meteotsunamis have been documented for events occurring in higher latitudes (de Jong and
1174 Battjes 2004; Wertman et al. 2014; Bechle et al. 2016), including the squall line of 1929 upon
1175 which Proudman developed his resonance theory (Proudman 1929). The existence of these
1176 additional generation mechanisms, other than wave-duct or wave-CISK, in the Mediterranean
1177 and Black Seas is worth investigating.

1178

1179 B.4. Importance of orography in generating meteotsunamigenic disturbances. One important
1180 question is to understand how significantly meteotsunamigenic disturbances are affected by
1181 high orography such as the Apennines and Alps located ca. 200-400 km from the
1182 meteotsunami hot spots in the Adriatic Sea (e.g., Belušić et al. 2007) or the Atlas Mountains
1183 (north Africa) close to the Balearic Islands. The quantification of the orography influence can
1184 be accessed via process-oriented numerical modelling studies that alter and/or remove the
1185 orography from the model and compare the physics of meteotsunamigenic disturbances
1186 reproduced with and without orography included.

1187

1188 B.5. Assessing meteotsunami potential in the future climate. Climate models are not capable
1189 to reproduce temporal and spatial scales of meteotsunamigenic disturbances; thus, they
1190 cannot be used for assessment of meteotsunamis in the future climate. However, there are
1191 indirect methods that might be used, such as using synoptic proxies (as done first for
1192 Ciutadella, Vilibić et al. 2018b) or using surrogate short-time simulations, where boundary
1193 conditions are changed to future climate scenarios by the so-called pseudo-global warming
1194 (PGW) methodology (Schär et al. 1996). The first method may be applied for meteotsunami
1195 hot spots where correlation is high between meteotsunamis and synoptic patterns, while the
1196 second approach is feasible for any meteotsunami hot spot, with reliability of results
1197 equivalent to the reliability of the regional climate model used.

1198

1199 B.6. Estimation of meteotsunami hazard and risk at hot spots. Meteotsunami hazard has been
1200 assessed for the Adriatic and Balearic sites (e.g., Vilibić et al. 2008; Orlić et al. 2010; Šepić et
1201 al. 2016a; Ličer et al. 2017; Denamiel et al. 2020), but not for other regions, such as
1202 southwestern Sicily coast and the Maltese Islands. Additionally, risk assessment has not been
1203 carried out for any of the Mediterranean and Black Sea hot spots, even for those which are

1204 known to regularly suffer from meteotsunami damage (Vučetić and Barčot, 2008; Vučetić et
1205 al. 2009). In addition, the risk to coastal infrastructure, goods, houses and other items is highly
1206 variable from one destructive meteotsunami event to the other. For example, in Vela Luka,
1207 which has become a highly touristic place in recent decades, the highest risk should be
1208 assessed by defining how much damage would be produced if an event similar to the
1209 meteotsunami of 21 June 1978 occurred today. This type of risk assessments should be
1210 developed at all locations where destructive meteotsunamis are known to occur.

1211

1212 B.7. Reducing meteotsunami hazard at hot spots. It is of highest importance to assess any
1213 interventions in coastal line and bathymetry at meteotsunami hot spots, as even small
1214 interventions and extensions may strongly change amplification characteristics and eigen
1215 oscillations of the bay or harbour (e.g., Marcos et al. 2005; Denamiel et al. 2018). Several
1216 solutions such as radial piers in a bay (Rabinovich 1992) may reduce the amplification factor
1217 and therefore the maximum wave height at the harbour head. However, such eventual
1218 interventions should be first assessed by targeted numerical modelling, as construction that
1219 narrows the entrance in a harbour or bay may even increase the amplification (Miles and
1220 Munk 1961; Rabinovich 2009).

1221

1222 B.8. Development and verification of meteotsunami early warning systems. Currently, only
1223 two meteotsunami early warning systems are available for the Mediterranean and Black Seas:
1224 in the middle Adriatic and the Balearic Islands. Simultaneously, the research is providing new
1225 and cost-effective methodologies that might be used to improve meteotsunami forecast,
1226 focusing exclusively on important meteotsunamigenic parameters (Romero et al. 2019). All
1227 these concepts might be used to improve the present meteotsunami early warning systems
1228 and their extension to other meteotsunami hot spots. Naturally, a catalogue of meteotsunami
1229 events or long-term high-frequency sea level measurements should be available at these sites
1230 first.

1231

1232 B.9. Assessing socio-economic aspects of meteotsunamis. The impact of meteotsunamis to
1233 coastal communities, including their reactions to the hazard, awareness of the hazards,
1234 development of societal services, mitigation and adaptation measures, at the level of the
1235 community as well as on the level of individuals, has not been researched in the

1236 Mediterranean and Black seas. Such research could be carried out for all meteotsunami hot
1237 spots and then the societal parameters could be intercompared and used to improve the
1238 related societal services.

1239

1240 **7. Concluding remarks**

1241

1242 This review is the first attempt to present meteotsunami research in the
1243 Mediterranean and Black Seas, a region in which these extreme events have traditionally been
1244 studied over the last 40 years. All meteotsunami aspects are presented, including several of
1245 ideas for future developments that may help researchers not only in this region but also
1246 worldwide. In addition, an initial bibliographical review has been performed, which will
1247 hopefully be extended globally in more comprehensive future studies.

1248 It should be emphasized here that observational networks are crucial in geosciences
1249 and should be further developed in the Mediterranean Sea to better understand, quantify and
1250 detect the hazards posed by meteotsunami events, which are likely to increase in frequency
1251 and intensity under climate change (Vilibić et al. 2018b). However, because of the cost of such
1252 systems (particularly the long-term cost of maintenance and repair) and the lack of funding
1253 dedicated to the sustainability of oceanographic observational networks, there is doubt about
1254 how research institutes will be able to maintain and further develop these networks. A way
1255 forward may be building up targeted networks with cheaper sensors, which will become
1256 available with future technological developments, while fulfilling the specific standard
1257 (resolution, precision, long-term stability) for measuring meteotsunamis. Aside from
1258 measurements, the growing application of numerical models at high resolutions in
1259 meteotsunami research is a great opportunity for model developments, which are generally
1260 based on finding new solutions to reproduce non-standard processes (i.e., processes at the
1261 edge of reproducibility). Hopefully, future development of meteotsunami tools and the
1262 research in the Mediterranean and Black Seas will follow these directions.

1263 This review is intended primarily for oceanographers, atmospheric scientists and ocean
1264 engineers, but meteotsunami research is a comprehensive subject that requires much wider
1265 competences, i.e., of mathematicians, statisticians, coastal managers, economists, policy
1266 makers, and more. The societal benefits of this research should be properly acknowledged in

1267 the future, as a gap between research and societal needs still exists. We expect that this
1268 review will eventually help to better connect research with society.

1269

1270

1271 **Acknowledgements:** To all scientists that contributed to the important research presented in
1272 this overview, and to all engineers and technicians that were engaged in data collections and
1273 data products which helped the meteotsunami research. The comments raised by two
1274 anonymous reviewers are greatly appreciated. This review has been supported by the project
1275 ADIOS of the Croatian Science Foundation (grant no. IP-2016-06-1955).

1276

1277 **Conflict of Interest:** The authors declare that they have no conflict of interest.

1278

1279 **References**

1280

1281 Airy GB (1878) On the tides at Malta. *Philos Trans R Soc Lond* 169: 123-138.

1282

1283 André G, Marcos M, Daubord C (2013) Detection method of meteotsunami events and
1284 characterization of harbor oscillations in Western Mediterranean. *Coastal Dynamics 2013*
1285 conference proceedings, 24–28 June 2013, pp. 83–92.

1286

1287 Angove M, Arcas D, Bailey R, et al (2019) Ocean observations required to minimize
1288 uncertainty in global tsunami forecasts, warnings, and emergency response. *Front Mar Sci* 6:
1289 350. <https://doi.org/10.3389/fmars.2019.00350>

1290

1291 Bechle AJ, Wu CH, Kristovich DAR, Anderson EJ, Schwab DJ, Rabinovich AB (2016)
1292 Meteotsunamis in the Laurentian Great Lakes. *Sci Rep* 6: 37832.
1293 <https://doi.org/10.1038/srep37832>

1294

1295 Bedosti B (1980) Considerazioni sul maremoto adriatico (tsunami) del 21.6.1978.
1296 *Supplemento Bollettini Sismici Provv.*, 12-14-20. pp. 2–17 (in Italian).

1297

1298 Belušić D, Strelec Mahović N (2009) Detecting and following atmospheric disturbances with a
1299 potential to generate meteotsunamis in the Adriatic. *Phys Chem Earth* 34: 918-927.
1300 <https://doi.org/10.1016/j.pce.2009.08.009>

1301

1302 Belušić D, Grisogono B, Klaić ZB (2007) Atmospheric origin of the devastating coupled air–sea
1303 event in the east Adriatic. *J Geophys Res* 112: D17111.
1304 <https://doi.org/10.1029/2006JD008204>

1305

1306 Brock JC, Purkis SJ (2009) The emerging role of lidar remote sensing in coastal research and
1307 resource management. *J Coast Res* 25: 1-5. <https://doi.org/10.2112/SI53-001.1>

1308

1309 Bubalo M, Janeković I, Orlić M (2018) Chrystal and Proudman resonances simulated with
1310 three numerical models. *Ocean Dyn* 68: 497-507. [https://doi-org/10.1007/s10236-018-1146-](https://doi-org/10.1007/s10236-018-1146-8)
1311 [8](https://doi-org/10.1007/s10236-018-1146-8)
1312
1313 Bubalo M, Janeković I, Orlić M (2019) Simulation of flooding and drying as an essential
1314 element of meteotsunami modelling. *Cont Shelf Res* 184: 81-90.
1315 <https://doi.org/10.1016/j.csr.2019.07.003>
1316
1317 Caloi P (1938) Sesse dell'alto Adriatico con particolare riguardo al Golfo di Trieste. *Memorie,*
1318 *R. Comitato Talassografico Italiano* 247: 1–39.
1319
1320 Candela J, Mazzola S, Sammari C, et al (1999) The “Mad Sea” phenomenon in the Strait of
1321 Sicily. *J Phys Oceanogr* 29: 2210–2231. [https://doi.org/10.1175/1520-](https://doi.org/10.1175/1520-0485(1999)029<2210:TMSPIT>2.0.CO;2)
1322 [0485\(1999\)029<2210:TMSPIT>2.0.CO;2](https://doi.org/10.1175/1520-0485(1999)029<2210:TMSPIT>2.0.CO;2)
1323
1324 Churchill DD, Houston SH, Bond NA (1995) The Daytona Beach wave of 3–4 July 1992: a
1325 shallow water gravity wave forced by a propagating squall line. *Bull Am Meteorol Soc* 76: 21-
1326 32. [https://doi.org/10.1175/1520-0477\(1995\)076<0021:TDBWOJ>2.0.CO;2](https://doi.org/10.1175/1520-0477(1995)076<0021:TDBWOJ>2.0.CO;2)
1327
1328 Colucci P, Michelato A (1976) An approach to the study of the “Marrubbio” phenomenon.
1329 *Boll Geof Teor Appl* 19: 3–10.
1330
1331 de Jong MPC, Battjes JA (2004). Low-frequency sea waves generated by atmospheric
1332 convection cells. *J Geophys Res* 109: C01011, <https://doi.org/10.1029/2003JC001931>
1333
1334 Defant A (1961) *Physical Oceanography*, Vol. 2, Pergamon Press, Oxford.
1335
1336 Denamiel C, Šepić J, Vilibić I (2018) Impact of geomorphological changes to harbor resonance
1337 during meteotsunamis: The Vela Luka Bay test case. *Pure Appl Geophys* 175: 3839-3859.
1338 <https://doi.org/10.1007/s00024-018-1862-5>
1339

1340 Denamiel C, Šepić J, Ivanković D, Vilibić I. (2019a) The Adriatic Sea and Coast modelling suite:
1341 Evaluation of the meteotsunami forecast component. Ocean Model 135: 71-93.
1342 <https://doi.org/10.1016/j.ocemod.2019.02.003>
1343

1344 Denamiel C, Šepić J, Huan X, Bolzer C, Vilibić I (2019b) Stochastic surrogate model for
1345 meteotsunami early warning system in the eastern Adriatic Sea. J Geophys Res Oceans 124:
1346 8485-8499. <https://doi.org/10.1029/2019JC015574>
1347

1348 Denamiel C, Šepić J, Huan X, Vilibić I (2020) Uncertainty propagation using polynomial chaos
1349 expansions for extreme sea level hazard assessment: the case of the eastern Adriatic
1350 meteotsunamis. J Phys Oceanogr 50: 1005-2021. <https://doi.org/10.1175/JPO-D-19-0147.1>
1351

1352 Dragani WC, D'Onofrio EE, Oreiro F, Alonso G, Fiore M, Grismeyer W (2014) Simultaneous
1353 meteorological tsunamis and storm surges at Buenos Aires coast, southeastern South
1354 America. Nat Hazards 74: 269-280. <https://doi.org/10.1007/s11069-013-0836-2>
1355

1356 Drago AF (2008) Numerical modelling of coastal seiches in Malta. Phys Chem Earth 3-4: 260-
1357 275. <https://doi.org/10.1016/j.pce.2007.02.001>
1358

1359 Drago AF (2009) Sea level variability and the 'Milghuba' seiche oscillations in the northern
1360 coast of Malta, Central Mediterranean. Phys Chem Earth 34: 948-970.
1361 <https://doi.org/10.1016/j.pce.2009.10.002>
1362

1363 Dusek G, DiVeglio C, Licate L, et al (2019) A meteotsunami climatology along the U.S. East
1364 Coast. Bull Am Meteor Soc 100: 1329-1345. <https://doi.org/10.1175/BAMS-D-18-0206.1>
1365

1366 Ewing M, Press F, Donn WJ (1954) An explanation of the Lake Michigan wave of 26 June
1367 1954. Science 120: 684-686. <https://doi.org/10.1126/science.120.3122.684>
1368

1369 Fontseré E. (1934) Les 'seixes' de la costa catalana. Servei Meteorologic de Catalunya, Notes
1370 d'Estudi (in Catalan).
1371

1372 Garcia-Soto C, van der Meeren GI, Busch JA, et al (2017) Advancing Citizen Science for
1373 Coastal and Ocean Research. French, V., Kellett, P., Delany, J., McDonough, N. [Eds.],
1374 Position Paper 23 of the European Marine Board, Ostend, Belgium. 112pp.
1375
1376 Garcies M, Gomis D, Monserrat S (1996) Pressure-forced seiches of large amplitude in inlets
1377 of the Balearic Islands: 2. Observational study. J Geophys Res 101: 6453-6467.
1378 <https://doi.org/10.1029/95JC03626>
1379
1380 Garrett CJR (1970) A theory of the Krakatoa tide gauge disturbances. Tellus 22: 43–52.
1381 <https://doi.org/10.1111/j.2153-3490.1970.tb01935.x>
1382
1383 Gomis D, Monserrat S, Tintoré J (1993) Pressure-forced seiches of large amplitude in inlets of
1384 the Balearic Islands. J Geophys Res 98: 14437-14445. <https://doi.org/10.1029/93JC00623>
1385
1386 Greenspan HP (1956) The generation of edge waves by moving pressure disturbances. J Fluid
1387 Mech 1: 574-592. <https://doi.org/10.1017/S002211205600038X>
1388
1389 Gusiakov VK, Dunbar PK, Arcos N (2019) Twenty-five years (1992–2016) of global tsunamis:
1390 Statistical and analytical overview. Nat Hazards 176: 2795–2807.
1391 <https://doi.org/10.1007/s00024-019-02113-7>
1392
1393 Haslett SK, Mellor HE, Bryant EA (2009) Meteo-tsunami hazard associated with summer
1394 thunderstorms in the United Kingdom. Phys Chem Earth 34: 1016-1022.
1395 <https://doi.org/10.1016/j.pce.2009.10.005>
1396
1397 Heidarzadeh M, Šepić J, Rabinovich A, Allahyar M, Soltanpour A, Tavakoli F (2020)
1398 Meteorological tsunami of 19 March 2017 in the Persian Gulf: Observations and analyses.
1399 Pure Appl Geophys 177: 1231-1259. <https://doi.org/10.1007/s00024-019-02263-8>
1400
1401 Heslop E, Tintoré J, Rotllan P, et al (2019) SOCIB integrated multi-platform ocean observing
1402 and forecasting; from ocean data to sector focused delivery of products and services. J Oper
1403 Oceanogr 2019: 1582129. <https://doi.org/10.1080/1755876X.2019.1582129>

1404

1405 Hibiya T, Kajiura K (1982) Origin of 'Abiki' phenomenon (a kind of seiche) in Nagasaki Bay. J
1406 Oceanogr Soc Japan 38: 172–182. <https://doi.org/10.1007/BF02110288>

1407

1408 Hodžić M (1979/1980) Occurrences of exceptional sea level oscillations in the Vela Luka Bay.
1409 Priroda (in Croatian) 68(2–3): 52–53.

1410

1411 Honda K, Terada T, Yoshida Y, Isitani D (1908) An investigation on the secondary undulations
1412 of oceanic tides. J College Sci, Imper Univ Tokyo, 108 p.

1413

1414 Horvath K, Vilibić I (2014) Atmospheric mesoscale conditions during the Boothbay
1415 meteotsunami: a numerical sensitivity study using a high-resolution mesoscale model. Nat
1416 Hazards 74: 55-74. <https://doi.org/10.1007/s11069-014-1055-1>

1417

1418 Horvath K, Šepić J, Telišman Prtenjak M (2018) Atmospheric forcing conducive for the
1419 Adriatic 25 June 2014 meteotsunami event. Pure Appl Geophys 175: 3817-3837.
1420 <https://doi.org/10.1007/s00024-018-1902-1>

1421

1422 Iglesias O, Lastras G, Souto C, Costa S, Canals M (2014) Effects of coastal submarine canyons
1423 on tsunami propagation and impact. Mar Geol 350: 39-51.
1424 <https://doi.org/10.1016/j.margeo.2014.01.013>

1425

1426 Jansà A (1986) Respuesta marina a perturbaciones mesometeorológicas: la "rissaga" de 21
1427 de junio de 1984 en Ciutadella (Menorca). Rev Meteorología, junio: 5-29 (in Spanish).

1428

1429 Jansà A (1987) Formulación y verificación de predicciones probabilísticas. Análisis del
1430 sistema de alertas meteorológicas. Servicio de predicción de rissagues y campaña Previmet
1431 Mediterráneo 87. Rev Meteorología (AME) 3(10): 5-11 (in Spanish)

1432

1433 Jansà A, Monserrat S, Gomis D (2007) The rissaga of 15 June 2006 in Ciutadella (Menorca), a
1434 meteorological tsunami. Adv Geosci 12: 1–4. <https://doi.org/10.5194/adgeo-12-1-2007>

1435

1436 Kim MS, Kim H, Eom HM, Yoo SH, Woo SB (2019) Occurrence of hazardous meteotsunamis
1437 coupled with pressure disturbance traveling in the Yellow Sea, Korea. J Coast Res SI91: 71-
1438 75. <https://doi.org/10.2112/SI91-015.1>
1439
1440 Lalaurette F (2002) Early detection of abnormal weather conditions using a probabilistic
1441 extreme forecast index. Q J R Meteorol Soc 129: 3037-3057.
1442 <https://doi.org/10.1256/qj.02.152>
1443
1444 Laprise R (1992) The Euler equations of motion with hydrostatic pressure as independent
1445 variable. Mon Wea Rev 120: 197-207. [https://doi.org/10.1175/1520-
1446 0493\(1992\)120<0197:TEEOMW>2.0.CO;2](https://doi.org/10.1175/1520-0493(1992)120<0197:TEEOMW>2.0.CO;2)
1447
1448 Ličer M, Mourre B, Troupin C, Krietemeyer A, Jansá A, Tintoré J (2017) Numerical study of
1449 Balearic meteotsunami generation and propagation under synthetic gravity wave forcing.
1450 Ocean Model 111: 38-45. <https://doi.org/10.1016/j.ocemod.2017.02.001>
1451
1452 Linares Á, Bechle AJ, Wu CH (2016) Characterization and assessment of the meteotsunami
1453 hazard in northern Lake Michigan. J Geophys Res Oceans 121: 7141-7158.
1454 <https://doi.org/10.1002/2016JC011979>
1455
1456 Linares Á, Wu CH, Bechle AJ, Anderson EJ, Kristovich DAR (2019) Unexpected rip currents
1457 induced by a meteotsunami. Sci Rep 9: 2105. <https://doi.org/10.1038/s41598-019-38716-2>
1458
1459 Lindzen RS, Tung K-K (1976) Banded convective activity and ducted gravity waves. Mon Wea
1460 Rev 104: 1602-1617. <https://doi.org/10.1029/2018JD029523>
1461
1462 Lipa B, Parikh H, Barrick D, Roarty H, Glenn S (2014) High-frequency radar observations of
1463 the June 2013 US East Coast meteotsunami. Nat Hazards 74: 109-122.
1464 <https://doi.org/10.1007/s11069-013-0992-4>
1465
1466 Liu PLF, Monserrat S, Marcos M (2002) Analytical simulation of edge waves observed around
1467 the Balearic Islands. Geophys Res Lett 29: 1847. <https://doi.org/10.1029/2002GL015555>

1468

1469 Liu PLF, Monserrat S, Marcos M, Rabinovich AB (2003) Coupling between two inlets:
1470 Observation and modelling. *J Geophys Res* 108: 3069.
1471 <https://doi.org/10.1029/2002JC001478>
1472

1473 Luettich RA, Birkhahn RH, Westerink JJ (1991) Application of ADCIRC-2DDI to
1474 Masonboro Inlet, North Carolina: a brief numerical modeling study. In: Contractors
1475 Report to the US Army Engineer Waterways Experiment Station, August 1991.
1476

1477 Marcos M, Monserrat S, Medina R, Vidal C (2003) Influence of the atmospheric wave velocity
1478 in the coastal amplification of meteotsunamis. *In: Submarine Landslides and Tsunamis* (Eds.
1479 A. C. Yalçiner, E. Pelinovsky, C. E. Synolakis, E. Okal), 247-253, Kluwer Academic Publishers,
1480 Amsterdam.
1481

1482 Marcos M, Liu PLF, Monserrat S (2004) Nonlinear resonant coupling between two adjacent
1483 bays. *J Geophys Res* 109: C05008. <https://doi.org/10.1029/2003JC002039>
1484

1485 Marcos M, Monserrat S, Medina R, Lomónaco P (2005) Response of a harbor with two
1486 connected basins to incoming long waves. *Appl Ocean Res* 27: 209-215.
1487 <https://doi.org/10.1016/j.apor.2005.11.010>
1488

1489 Marcos M, Monserrat S, Medina R, Orfila A, Olabarrieta M (2009) External forcing of
1490 meteorological tsunamis at the coast of the Balearic Islands. *Phys Chem Earth* 17-18: 838-
1491 947. <https://doi.org/10.1016/j.pce.2009.10.001>
1492

1493 Marques J, Lopes B, Ferreira C, et al (2019) Towards a practical and cost-effective water
1494 monitoring system. In: Camarinha-Matos L., Almeida R., Oliveira J. (eds) *Technological
1495 Innovation for Industry and Service Systems. DoCEIS 2019. IFIP Advances in Information and
1496 Communication Technology*, vol 553. Springer, Cham. [https://doi.org/10.1007/978-3-030-
1497 17771-3_23](https://doi.org/10.1007/978-3-030-17771-3_23)
1498

1499 Medvedev I, Vilibić I, Rabinovich AB (2020) Tidal resonance in the Adriatic Sea: Observational
1500 evidence. *J Geophys Res Oceans* 125: e2020JC016168.
1501 <https://doi.org/10.1029/2020JC016168>
1502

1503 Metzner M, Gade M, Hennings I, Rabinovich AB (2000) The observation of seiches in the
1504 Baltic Sea using a multi data set of water levels. *J Mar Syst* 24: 67-84.
1505 [https://doi.org/10.1016/S0924-7963\(99\)00079-2](https://doi.org/10.1016/S0924-7963(99)00079-2)
1506

1507 Miles J, Munk W (1961) Harbor paradox. *J Waterw Harbor Div ASCE* 87: 111–132.
1508

1509 Monserrat S, Thorpe AJ (1992) Gravity-wave observations using an array of microbarographs
1510 in the Balearic Islands. *Quart J Roy Meteorol Soc* 118: 259-282.
1511 <https://doi.org/10.1002/qj.49711850405>
1512

1513 Monserrat S, Thorpe AJ (1996) Use of ducting theory in an observed case of gravity waves. *J*
1514 *Atmos Sci* 53: 1724-1736. [https://doi.org/10.1175/1520-](https://doi.org/10.1175/1520-0469(1996)053<1724:UODTIA>2.0.CO;2)
1515 [0469\(1996\)053<1724:UODTIA>2.0.CO;2](https://doi.org/10.1175/1520-0469(1996)053<1724:UODTIA>2.0.CO;2)
1516

1517 Monserrat S, Ibberson A, Thorpe AJ (1991a) Atmospheric gravity waves and the “rissaga”
1518 phenomenon, *Quart J Roy Meteorol Soc* 117: 553–570.
1519 <https://doi.org/10.1002/qj.49711749907>
1520

1521 Monserrat S, Ramis C, Thorpe AJ (1991b) Large-amplitude pressure oscillations in the
1522 Western Mediterranean. *Geophys Res Lett* 18: 183-186. <https://doi.org/10.1029/91GL00234>
1523

1524 Monserrat S, Rabinovich AB, Casas B (1998) On the reconstruction of the transfer function
1525 for atmospherically generated seiches. *Geophys Res Lett* 25: 2197-2200.
1526 <https://doi.org/10.1029/98GL01506>
1527

1528 Monserrat S, Vilibić I, Rabinovich AB (2006) Meteotsunamis: atmospherically induced
1529 destructive ocean waves in the tsunami frequency band. *Nat Hazards Earth Syst Sci* 6: 1035-
1530 1051. <https://doi.org/10.5194/nhess-6-1035-2006>

1531

1532 Nakano M, Unoki S (1962) On the seiches (secondary undulations of tides) along the coast of
1533 Japan. Records Oceanogr Works Japan, Spec No 6: 169-214.

1534

1535 Okal EA, Synolakis CE (2008) Far-field tsunami hazard from mega-thrust earthquakes in the
1536 Indian Ocean. Geophys J Internat 172: 995–1015. [https://doi.org/10.1111/j.1365-
1537 246X.2007.03674.x](https://doi.org/10.1111/j.1365-246X.2007.03674.x)

1538

1539 Okal EA, Visser JNJ, de Beer CH (2014) The Dwarskersbos, South Africa local tsunami of
1540 August 27, 1969: field survey and simulation as a meteorological event. Nat Hazards 74: 251-
1541 268. <https://doi.org/10.1007/s11069-014-1205-5>

1542

1543 Olabarrieta M, Valle-Levinson A, Martinez CJ, Pattiaratchi C, Shi L (2017) Meteotsunamis in
1544 the northeastern Gulf of Mexico and their possible link to El Niño Southern Oscillation. Nat
1545 Hazards 88: 1325-1346. <https://doi.org/10.1007/s11069-017-2922-3>

1546

1547 Orfila A, Balle S, Simarro G (2011) Topographic enhancement of long waves generated by an
1548 idealized moving pressure system. Sci Mar 75: 595-693.
1549 <https://doi.org/10.3989/scimar.2011.75n3595>

1550

1551 Orlić M (1980) About a possible occurrence of the Proudman resonance in the Adriatic.
1552 Thalassia Jugoslav 16(1): 79-88.

1553

1554 Orlić M (2015) The first attempt at cataloguing tsunami-like waves of meteorological origin
1555 in Croatian coastal waters. Acta Adriat 56(1): 83–96.

1556

1557 Orlić M, Belušić D, Janeković I, Pasarić M (2010) Fresh evidence relating the great Adriatic
1558 surge of 21 June 1978 to mesoscale atmospheric forcing. J Geophys Res 115: C06011.
1559 <https://doi.org/10.1029/2009JC005777>

1560

1561 Pattiaratchi CB, Wijeratne EMS (2014) Observations of meteorological tsunamis along the
1562 south-west Australian coast. Nat Hazards 74: 281-303. [https://doi.org/10.1007/s11069-014-](https://doi.org/10.1007/s11069-014-1263-8)
1563 [1263-8](https://doi.org/10.1007/s11069-014-1263-8)
1564
1565 Pattiaratchi CB, Wijeratne EMS (2015) Are meteotsunamis an underrated hazard? Philos
1566 Trans R Soc A 373: 20140377. <https://doi.org/10.1098/rsta.2014.0377>
1567
1568 Paxton CH, Sobien DA (1998) Resonant interaction between an atmospheric gravity wave
1569 and shallow water wave along Florida's west coast. Bull Am Meteorol Soc 79: 2727-2732.
1570 [https://doi.org/10.1175/1520-0477\(1998\)079<2727:RIBAAG>2.0.CO;2](https://doi.org/10.1175/1520-0477(1998)079<2727:RIBAAG>2.0.CO;2)
1571
1572 Pellikka H, Rauhala J, Kahma KK, Stipa T, Boman H, Kangas A (2014) Recent observations of
1573 meteotsunamis on the Finnish coast. Nat Hazards 74: 197-215.
1574 <https://doi.org/10.1007/s11069-014-1150-3>
1575
1576 Petroliağis TI, Pinson P (2012) Early indication of extreme winds utilizing the Extreme
1577 Forecast Index. In: ECMWF Newsletter 132, pp. 13-19 (Summer 2012).
1578
1579 Picco P, Schiano ME, Incardone S, et al (2019) Detection and characterization of
1580 meteotsunamis in the Gulf of Genoa. J Mar Sci Eng 7: 275.
1581 <https://doi.org/10.3390/jmse7080275>
1582
1583 Pinardi N, Coppini G (2010) Operational oceanography in the Mediterranean Sea: the
1584 second stage of development. Ocean Sci 6: 263–267. <https://doi.org/10.5194/os-6-263-2010>
1585
1586 Pinardi N, Allen I, Demirov E, et al (2003) The Mediterranean ocean forecasting
1587 system: first phase of implementation (1998–2001). Ann Geophys 21: 3–20.
1588 <https://doi.org/10.5194/angeo-21-3-2003>
1589
1590 Plougonven R, Zhang F (2014) Internal gravity waves from atmospheric jets and fronts.
1591 Rev Geophys 52: 33-76. <https://doi.org/10.1002/2012RG000419>
1592

1593 Powers JG, Reed RJ (1993) Numerical simulation of the large-amplitude mesoscale gravity-
1594 wave event of 15 December 1987 in the central United States. *Mon Wea Rev* 121: 2285-
1595 2308. [https://doi.org/10.1175/1520-0493\(1993\)121<2285:NSOTLA>2.0.CO;2](https://doi.org/10.1175/1520-0493(1993)121<2285:NSOTLA>2.0.CO;2)
1596
1597 Proudman J (1929) The effects on the sea of changes in atmospheric pressure. *Geophys*
1598 *Suppl Mon Not R Astron Soc* 2(4): 197–209. [https://doi.org/10.1111/j.1365-
1599 246X.1929.tb05408.x](https://doi.org/10.1111/j.1365-246X.1929.tb05408.x)
1600
1601 Rabinovich AB (1992) Possible vorticity effect in longwave motions (surging) in harbors,
1602 *Trans (Doklady) Russian Acad Scie, Earth Sci Sec* 325: 224–228.
1603
1604 Rabinovich AB (1993) Long Ocean Gravity Waves: Trapping, Resonance, and Leaking,
1605 *Gidrometeoizdat, St. Petersburg*, 325 pp. (in Russian).
1606
1607 Rabinovich AB (1997) Spectral analysis of tsunami waves: Separation of source and
1608 topography effects. *J Geophys Res* 102: 12663–12676. <https://doi.org/10.1029/97JC00479>
1609
1610 Rabinovich AB (2009) Seiches and harbour oscillations. In Y. C. Kim (Ed.), *Handbook of*
1611 *coastal and ocean engineering* (pp. 193–236). Singapore: World Scientific.
1612 https://doi.org/10.1142/9789812819307_0009
1613
1614 Rabinovich AB (2020) Twenty-seven years of progress in the science of meteorological
1615 tsunamis following the 1992 Daytona Beach event. *Pure Appl Geophys* 177: 1193-1230.
1616 <https://doi.org/10.1007/s00024-019-02349-3>
1617
1618 Rabinovich AB, Monserrat S (1996) Meteorological tsunamis near the Balearic and Kuril
1619 Islands: descriptive and statistical analysis. *Nat Hazards* 13: 55-90.
1620 <https://doi.org/10.1007/BF00156506>
1621
1622 Rabinovich AB, Monserrat S (1998) Generation of meteorological tsunamis (large amplitude
1623 seiches) near the Balearic and Kuril islands. *Nat Hazards* 18: 27-55.
1624 <https://doi.org/10.1023/A:1008096627047>

1625

1626 Rabinovich AB, Monserrat S, Fine IV (1999) Numerical modeling of extreme seiche
1627 oscillations in vicinity of the Balearic Islands. *Okeanologiya* 39: 16-24.

1628

1629 Rabinovich AB, Vilibić I, Tinti S (2009) Meteorological tsunamis: atmospherically induced
1630 destructive ocean waves in the tsunami frequency band. *Phys Chem Earth* 34: 891-893.
1631 <https://doi.org/10.1016/j.pce.2009.10.006>

1632

1633 Rabinovich AB, Šepić J, Thomson RE (2020) The meteorological tsunami of 1 November 2010
1634 in the southern Strait of Georgia: A case study. *Nat Hazards* (this issue).

1635

1636 Ramis C, Jansà A (1983) Condiciones meteorológicas simultáneas a la aparición de
1637 oscilaciones del nivel del mar de amplitud extraordinaria en el Mediterráneo occidental, *Rev*
1638 *Geofísica* (in Spanish) 39: 35-42.

1639

1640 Renault L, Vizoso G, Jansà A, Wilkin J, Tintoré J (2011) Toward the predictability of
1641 meteotsunamis in the Balearic Sea using regional nested atmosphere and ocean models.
1642 *Geophys Res Lett* 38: L10601. <https://doi.org/10.1029/2011GL047361>

1643

1644 Roarty H, Cook T, Hazard L, et al (2019) The global high frequency radar network. *Front Mar*
1645 *Sci* 6: 164. <https://doi.org/10.3389/fmars.2019.00164>

1646

1647 Romero R, Vich M, Ramis C (2019) A pragmatic approach for the numerical prediction of
1648 meteotsunamis in Ciutadella harbour (Balearic Islands). *Ocean Model* 142: 101441.
1649 <https://doi.org/10.1016/j.ocemod.2019.101441>

1650

1651 Salaree A, Mansouri R, Okal EA (2018) The intriguing tsunami of 19 March 2017 at Bandar
1652 Dayyer, Iran: field survey and simulations. *Nat Hazards* 90: 1277-1307.
1653 <https://doi.org/10.1007/s11069-017-3119-5>

1654

1655 Saltelli A, Ratto M, Andres T, et al (2008) *Global Sensitivity Analysis: The Primer*. John Wiley
1656 & Sons, 304 pp.

1657
1658 Schär C, Frei C, Luthi D, Davies HC (1996) Surrogate climate-change scenarios for regional
1659 925 climate models. *Geophys Res Lett* 23: 669–672. <https://doi.org/10.1029/96GL00265>
1660
1661 Šepić J, Vilibić I (2011) The development and implementation of a real-time meteotsunami
1662 warning network for the Adriatic Sea. *Nat Hazards Earth Syst Sci* 11: 83-91.
1663 <https://doi.org/10.5194/nhess-11-83-2011>
1664
1665 Šepić J, Rabinovich AB (2014) Meteotsunami in the Great Lakes and on the Atlantic coast of
1666 the United States generated by the “derecho” of June 29–30, 2012. *Nat Hazards* 74: 75-107.
1667 <https://doi.org/10.1007/s11069-014-1310-5>
1668
1669 Šepić J, Orlić M (2020) Catalogue of meteorological tsunamis in Croatian coastal waters.
1670 http://jadran.izor.hr/~seplic/meteotsunami_catalogue, accessed 10 July 2020
1671
1672 Šepić J, Orlić M, Vilibić I (2008) The Bakar Bay seiches and their relationship with
1673 atmospheric processes. *Acta Adriat* 49(2): 107-123.
1674
1675 Šepić J, Vilibić I, Monserrat S (2009a) Teleconnections between the Adriatic and the Balearic
1676 meteotsunamis. *Phys Chem Earth* 34: 928-937. <https://doi.org/10.1016/j.pce.2009.08.007>
1677
1678 Šepić J, Vilibić I, Belušić D (2009b) The source of the 2007 Ist meteotsunami (Adriatic Sea). *J*
1679 *Geophys Res Oceans* 114: C03016. <https://doi.org/10.1029/2008JC005092>
1680
1681 Šepić J, Vilibić I, Strelec Mahović N (2012) Northern Adriatic meteorological tsunamis:
1682 Observations, link to the atmosphere, and predictability. *J Geophys Res* 117: C02002.
1683 <https://doi.org/10.1029/2011JC007608>
1684
1685 Šepić J, Vilibić I, Rabinovich AB, Monserrat S (2015a) Widespread tsunami-like waves of 23-
1686 27 June in the Mediterranean and Black Seas generated by high-altitude atmospheric
1687 forcing. *Sci Rep* 5, 11682. <https://doi.org/10.1038/srep11682>
1688

1689 Šepić J, Vilibić I, Fine I (2015b) Northern Adriatic meteorological tsunamis: Assessment of
1690 their potential through ocean modeling experiments. *J Geophys Res Oceans* 120: 2993-2010.
1691 <https://doi.org/10.1002/2015JC010795>
1692

1693 Šepić J, Vilibić I, Lafon A, Macheboeuf L, Ivanović Z (2015c) High-frequency sea level
1694 oscillations in the Mediterranean and their connection to synoptic patterns. *Prog Oceanogr*
1695 137: 284-298. <https://doi.org/10.1016/j.pocean.2015.07.005>
1696

1697 Šepić J, Vilibić I, Monserrat S (2016a) Quantifying the probability of meteotsunami
1698 occurrence from synoptic atmospheric patterns. *Geophys Res Lett* 43: 10377-10384.
1699 <https://doi.org/10.1002/2016GL070754>
1700

1701 Šepić J, Međugorac I, Janeković I, Dunić N, Vilibić I (2016b) Multi-meteotsunami event in the
1702 Adriatic Sea generated by atmospheric disturbances of 25–26 June 2014. *Pure Appl Geophys*
1703 173: 4117-4138. <https://doi.org/10.1007/s00024-016-1249-4>
1704

1705 Šepić J, Vilibić I, Beg Paklar G, et al (2017) Towards an understanding and operational early
1706 warning of the Adriatic meteotsunamis: Project MESSI. Coastal and Maritime Mediterranean
1707 Conference, Split, Croatia, 29 November – 1 December 2017.
1708 <https://doi.org/10.5150/cmcm.2017.033>
1709

1710 Šepić J, Vilibić I, Rabinovich AB, Tinti S (2018a) Meteotsunami ("Marrobbio") of 25-26 June
1711 2014 on the southwestern coast of Sicily, Italy. *Pure Appl Geophys* 175: 1573-1593.
1712 <https://doi.org/10.1007/s00024-018-1827-8>
1713

1714 Šepić J, Rabinovich AB, Sytov VN (2018b) Odessa tsunami of 27 June 2014: Observations and
1715 numerical modelling. *Pure Appl Geophys* 175: 1545-1572. [https://doi.org/10.1007/s00024-](https://doi.org/10.1007/s00024-017-1729-1)
1716 [017-1729-1](https://doi.org/10.1007/s00024-017-1729-1)
1717

1718 Shchepetkin AF, McWilliams JC (2005) The regional oceanic modeling system: a split-explicit,
1719 free-surface, topography-following-coordinate ocean model. *Ocean Model* 9: 347–404.
1720 <https://doi.org/10.1016/j.ocemod.2004.08.002>

1721

1722 Shchepetkin AF, McWilliams JC (2009) Correction and commentary for “ocean forecasting
1723 in terrain-following coordinates: formulation and skill assessment of the regional
1724 ocean modeling system” by Haidvogel et al. J. Comput. Phys., 227, pp.
1725 3595–3624. J Comput Phys 228: 8985-9000. <https://doi.org/10.1016/j.jcp.2009.09.002>
1726

1727 Sheremet A, Gravois U, Shrira V (2016) Observations of meteotsunami on the Louisiana
1728 shelf: a lone soliton with a soliton pack. Nat Hazards 84: 471-492.
1729 <https://doi.org/10.1007/s11069-016-2446-2>
1730

1731 Shi LM, Olabarrieta M, Valle-Levinson A, Warner JC (2019) Relevance of wind stress and
1732 wave-dependent ocean surface roughness on the generation of winter meteotsunamis in the
1733 Northern Gulf of Mexico. Ocean Model 140: 101408.
1734 <https://doi.org/10.1016/j.ocemod.2019.101408>
1735

1736 Shi LM, Olabarrieta M, Nolan DS, Warner JC (2020) Tropical cyclone rainbands can trigger
1737 meteotsunamis. Nat Comm 11: 678. <https://doi.org/10.1038/s41467-020-14423-9>
1738

1739 Skamarock WC (2004) Evaluating mesoscale NWP models using kinetic energy spectra.
1740 Mon Wea Rev 132: 3019-3032. <https://doi.org/10.1175/MWR2830.1>
1741

1742 Skamarock WC, Klemp JB, Dudhia J, et al (2005) A description of the advanced research WRF
1743 version 2. In: NCAR
1744 Technical Note NCAR/TN-468+STR, <https://doi.org/10.5065/D6DZ069T>
1745

1746 Sobol’ IM (2001) Global sensitivity indices for nonlinear mathematical models and their
1747 Monte Carlo estimates. Math Comput Simul 55: 271-280. [https://doi.org/10.1016/S0378-
1748 4754\(00\)00270-6](https://doi.org/10.1016/S0378-4754(00)00270-6)
1749

1750 Soize C, Ghanem RG (2004) Physical systems with random uncertainties: Chaos
1751 representations with arbitrary probability measure. SIAM J Sci Comput 26: 395-410.
1752 <https://doi.org/10.1137/S1064827503424505>

1753

1754 Sterneck R (1914) Ueber 'Seiches' an den Kuesten der Adria. Sitzungsberichte, Akademie der
1755 Wissenschaften in Wien, Mathematisch-naturwissenschaftliche Klasse, 123, 2199–2232.

1756

1757 Sudret B (2008) Global sensitivity analysis using polynomial chaos expansions. Reliab Eng
1758 Syst Saf 93: 964-979. <https://doi.org/10.1016/j.ress.2007.04.002>

1759

1760 Tanaka K (2010) Atmospheric pressure-wave bands around a cold front resulted in a
1761 meteotsunami in the East China Sea in February 2009. Nat Hazards Earth Syst Sci 10: 2599-
1762 2610. <https://doi.org/10.5194/nhess-10-2599-2010>

1763

1764 Thomson RE, Rabinovich AB, Fine IV, et al (2009) Meteorological tsunamis on the coasts of
1765 British Columbia and Washington. Phys Chem Earth 34: 971-988.
1766 <https://doi.org/10.1016/j.pce.2009.10.003>

1767

1768 Tinti S, Graziani L, Brizuela B, Maramai A, Gallazzi S (2012) Applicability of the Decision
1769 Matrix of North Eastern Atlantic, Mediterranean and connected seas Tsunami Warning
1770 System to the Italian tsunamis. Nat Hazards Earth Syst Sci 12: 843–857.
1771 <https://doi.org/10.5194/nhess-12-843-2012>

1772

1773 Tintoré J, Gomis D, Alonso S, Wang DP (1988) A theoretical study of large sea level
1774 oscillations in the Western Mediterranean. J Geophys Res 93: 10797-10803.
1775 <https://doi.org/10.1029/JC093iC09p10797>

1776

1777 Tintoré J, Vizoso G, Casas B, et al (2013) SOCIB: The Balearic Islands coastal ocean observing
1778 and forecasting system responding to science, technology and society needs. Mar Technol
1779 Sci J 47: 101-117. <https://doi.org/10.4031/MTSJ.47.1.10>

1780

1781 Titov VV, Synolakis CE (1998) Numerical modeling of tidal wave runup. J Waterw Port C ASCE
1782 124: 157-191. [https://doi.org/10.1061/\(ASCE\)0733-950X\(1998\)124:4\(157\)](https://doi.org/10.1061/(ASCE)0733-950X(1998)124:4(157))

1783

1784 Tonani M, Teruzzi A, Korres G, et al (2014) The Mediterranean Monitoring and Forecasting
1785 Centre, a component of the MyOcean system. In: Dahlin, H., Fleming, N.C., Petersson, S.E.
1786 (Eds.), Proceedings of the Sixth International Conference on EuroGOOS 4–6 October 2011,
1787 Sopot, Poland, Eurogoos Publication no. 30.
1788

1789 Tsimplis MN, Proctor R, Flather RA (1995) A two-dimensional tidal model for the
1790 Mediterranean Sea. *J Geophys Res Oceans* 100: 16223-16239.
1791 <https://doi.org/10.1029/95JC01671>
1792

1793 Vennell R (2007) Long barotropic waves generated by a storm crossing topography. *J Phys*
1794 *Oceanogr* 37: 2809-2823. <https://doi.org/10.1175/2007JPO3687.1>
1795

1796 Vilibić I, Mihanović H (2003) A study of resonant oscillations in the Split harbour (Adriatic
1797 Sea). *Estuar Coast Shelf Sci* 56: 861-867. [https://doi.org/10.1016/S0272-7714\(02\)00304-9](https://doi.org/10.1016/S0272-7714(02)00304-9)
1798

1799 Vilibić I, Beg Paklar G (2006) High-frequency atmospherically-induced oscillations in the
1800 middle Adriatic coastal area. *Ann Geophys* 24: 2759-2771. [https://doi.org/10.5194/angeo-](https://doi.org/10.5194/angeo-24-2759-2006)
1801 [24-2759-2006](https://doi.org/10.5194/angeo-24-2759-2006)
1802

1803 Vilibić I, Šepić J (2009) Destructive meteotsunamis along the eastern Adriatic coast:
1804 Overview. *Phys Chem Earth* 34: 904-917. <https://doi.org/10.1016/j.pce.2009.08.004>
1805

1806 Vilibić I, Domijan N, Orlić M, Leder N, Pasarić M (2004) Resonant coupling of a traveling air-
1807 pressure disturbance with the east Adriatic coastal waters. *J Geophys Res Oceans* 109:
1808 C10001. <https://doi.org/10.1029/2004JC002279>
1809

1810 Vilibić I, Domijan N, Čupić S (2005) Wind versus air pressure seiche triggering in the Middle
1811 Adriatic coastal waters. *J Mar Syst* 57: 189-200.
1812 <https://doi.org/10.1016/j.jmarsys.2005.04.007>
1813

1814 Vilibić I, Monserrat S, Rabinovich AB, Mihanović H (2008) Numerical modelling of the
1815 destructive meteotsunami of 15 June 2006 on the coast of the Balearic Islands. Pure Appl
1816 Geophys 165: 2169-2195. <https://doi.org/10.1007/s00024-008-0426-5>
1817

1818 Vilibić I, Šepić J, Rangelov J, Strelec-Mahović N, Tinti S (2010) Possible atmospheric origin of
1819 the 7 May 2007 western Black Sea shelf tsunami event. J Geophys Res 115: C07006.
1820 <https://doi.org/10.1029/2009JC005904>
1821

1822 Vilibić I, Mihanović H, Charayre F (2014a) Assessing meteotsunami potential of high-
1823 frequency air pressure oscillations observed in the middle Adriatic. Nat Hazards 74: 217-232.
1824 <https://doi.org/10.1007/s11069-013-0865-x>
1825

1826 Vilibić I, Monserrat S, Rabinovich AB (2014b) Meteorological tsunamis on the US East Coast
1827 and in other regions of the World Ocean. Nat Hazards 74: 1–9.
1828 <https://doi.org/10.1007/s11069-014-1350-x>
1829

1830 Vilibić I, Horvath K, Strelec Mahović N, et al (2014c) Atmospheric processes responsible for
1831 generation of the 2008 Boothbay meteotsunami. Nat Hazards 74: 25-53.
1832 <https://doi.org/10.1007/s11069-013-0811-y>
1833

1834 Vilibić I, Šepić J, Rabinovich AB, Monserrat S (2016) Modern approaches in meteotsunami
1835 research and early warning. Front Mar Sci 3: 57. <https://doi.org/10.3389/fmars.2016.00057>
1836

1837 Vilibić I, Horvath K, Palau JL (2018a) Meteorology and climatology of the Mediterranean and
1838 Black seas: Introduction. Pure Appl Geophys 175: 3721-3725.
1839 <https://doi.org/10.1007/s00024-018-2021-8>
1840

1841 Vilibić I, Šepić J, Dunić N, Sevault F, Monserrat S, Jordà G (2018b) Proxy-based assessment of
1842 strength and frequency of meteotsunamis in future climate. Geophys Res Lett 45: 10501-
1843 10508. <https://doi.org/10.1029/2018GL079566>
1844

1845 Vučetić T, Barčot T (2008) Records of “tidal” wave in Vela Luka on 21 June 1978 (in Croatian),
1846 technical report, 80 pp, Municipality of Vela Luka, Institute of Oceanography and Fisheries,
1847 Vela Luka, Croatia.

1848

1849 Vučetić T, Vilibić I, Tinti S, Maramai A (2009) The Great Adriatic flood of 21 June 1978
1850 revisited: An overview of the reports. *Phys Chem Earth* 34: 894-903.
1851 <https://doi.org/10.1016/j.pce.2009.08.005>

1852

1853 Warner JC, Armstrong B, He R, Zambon JB (2010) Development of a coupled ocean-
1854 atmosphere-wave-sediment transport (COAWST) modeling system. *Ocean Model* 35: 230-
1855 244. <https://doi.org/10.1016/j.ocemod.2010.07.010>

1856

1857 Wertman CA, Yablonsky RM, Shen Y, Merrill J, Kincaid CR, Pockalny RA (2014) Mesoscale
1858 convective system surface pressure anomalies responsible for meteotsunamis along the US
1859 East Coast on June 13th, 2013. *Sci Rep* 4: 7143. <https://doi.org/10.1038/srep07143>

1860

1861 Williams DA, Horsburgh KJ, Schultz DM, Hughes CW (2019) Examination of generation
1862 mechanisms for an English Channel meteotsunami: Combining observations and modeling. *J*
1863 *Phys Oceanogr* 49: 103-120. <https://doi.org/10.1175/JPO-D-18-0161.1>

1864

1865 Williams DA, Horsburgh KJ, Schultz DM, Hughes CW (2020) Proudman resonance with tides,
1866 bathymetry and variable atmospheric forcings. *Nat Hazards*, in press.
1867 <https://doi.org/10.1007/s11069-020-03896-y>

1868

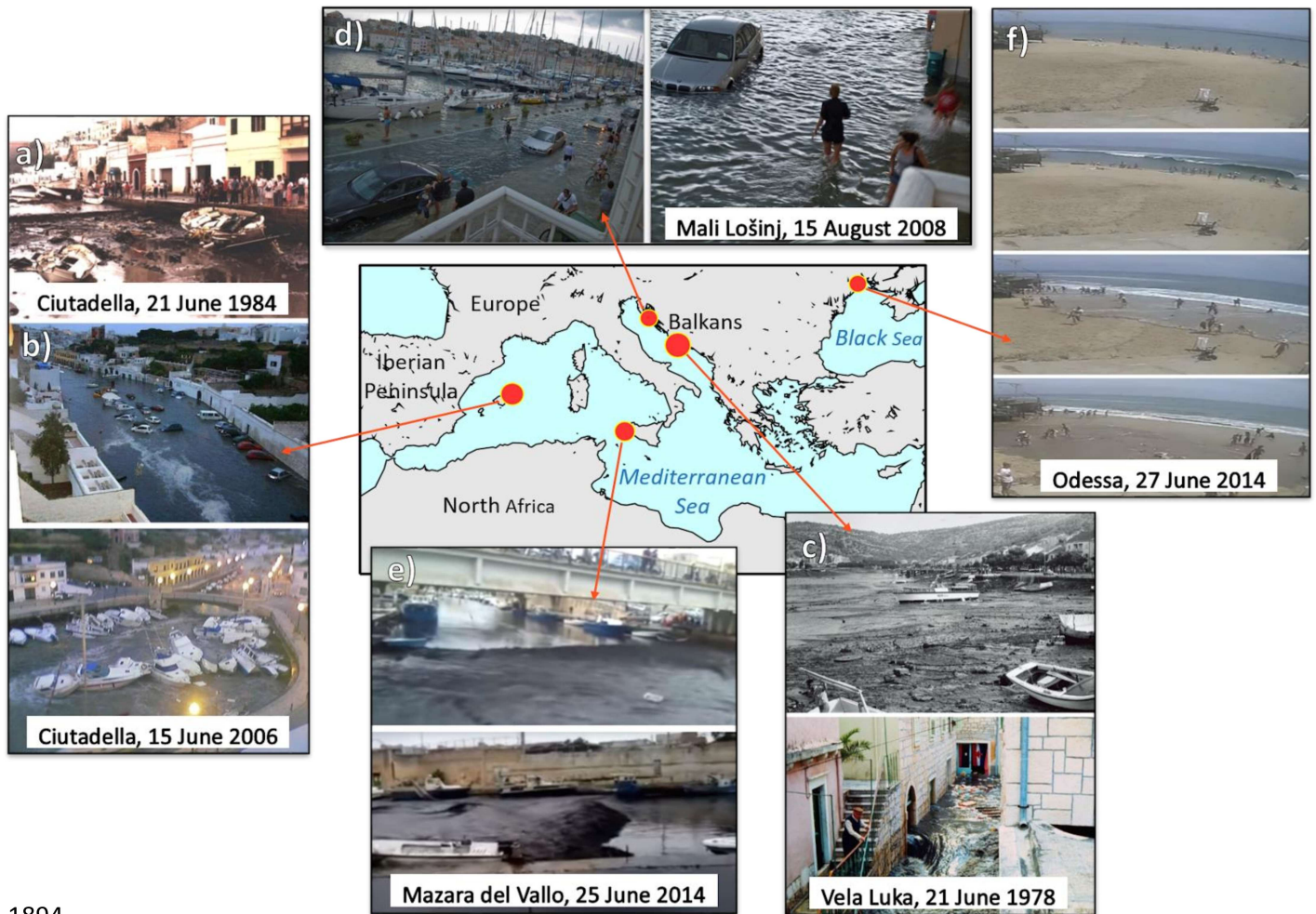
1869 Wilson BW (1972) Seiches. *Adv Hydrosoci* 8: 1–94. [https://doi.org/10.1016/B978-0-12-](https://doi.org/10.1016/B978-0-12-021808-0.50006-1)
1870 [021808-0.50006-1](https://doi.org/10.1016/B978-0-12-021808-0.50006-1)

1871

1872 Xiu D, Karniadakis GE (2002) Stochastic modeling of flow-structure interactions using
1873 generalized polynomial chaos. *J Fluids Eng* 124: 51-59. <https://doi.org/10.1115/1.1436089>

1874

1875 Yalçiner A, Pelinovsky E, Talipova T, Kurkin A, Kozelkov A, Zaitsev A (2004). Tsunamis in the
1876 Black Sea: Comparison of the historical, instrumental, and numerical data. J Geophys Res
1877 109: C12023. <https://doi.org/10.1029/2003JC002113>
1878
1879 Zemunik P, Bonanno A, Mazzola S, et al (2020) Observing meteotsunamis („Marrobbio“) in
1880 the southwestern coast of Sicily. Nat Hazards, accepted (this issue)
1881
1882 Zore-Armanda M (1979) Destructive wave in the Adriatic. Rapport et Procès-verbaux des
1883 Réunions du Conseil International pour l'Exploration Scientifique de la Mer Méditerranée
1884 25–26: 93–94.
1885
1886 Zsótér E (2006) Recent developments in extreme weather forecasting. ECMWF newsletter
1887 107. Spring 2006, 8–17.
1888
1889 Zsótér E, Pappenberger F, Richardson D (2014) Sensitivity of model climate to sampling
1890 configurations and the impact on the Extreme Forecast Index. Meteorol Appl 22: 236-257.
1891 <https://doi.org/10.1002/met.1447>
1892
1893



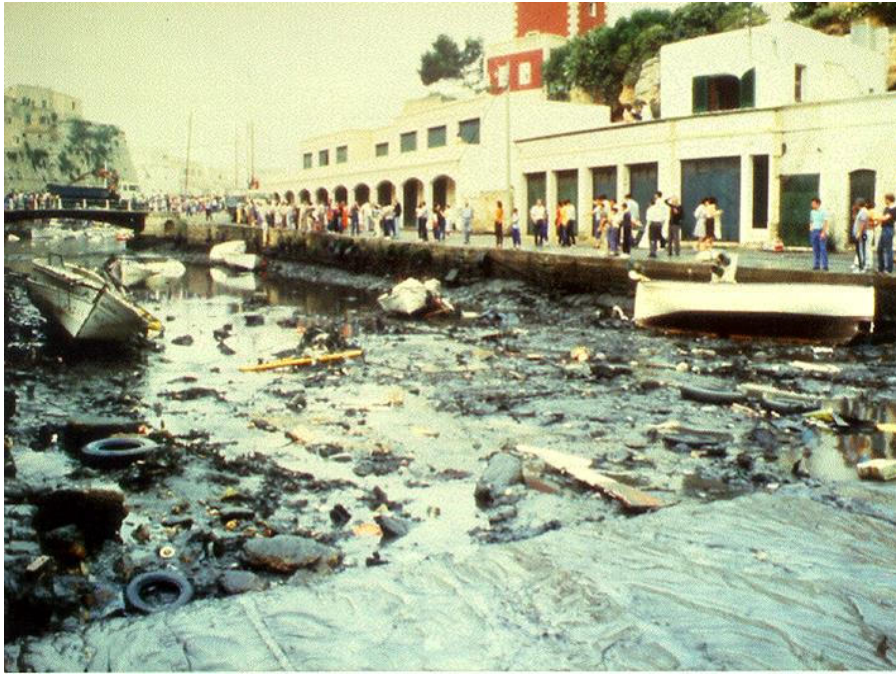
1894
1895
1896
1897
1898
1899
1900
1901

Figure 1. Locations (red circles) and photos of the most prominent meteotsunami events in the Mediterranean Sea: (a) the Balearic meteotsunamis of the 21 June 1984 and (b) 15 June 2006, (c) the middle Adriatic meteotsunamis of 21 June 1978, (d) the Mali Lošinj meteotsunamis of 15 August 2008, (e) the Mazara del Vallo meteotsunamis of 25 June 2014, and (f) the Odessa meteotsunamis of 27 June 2014.



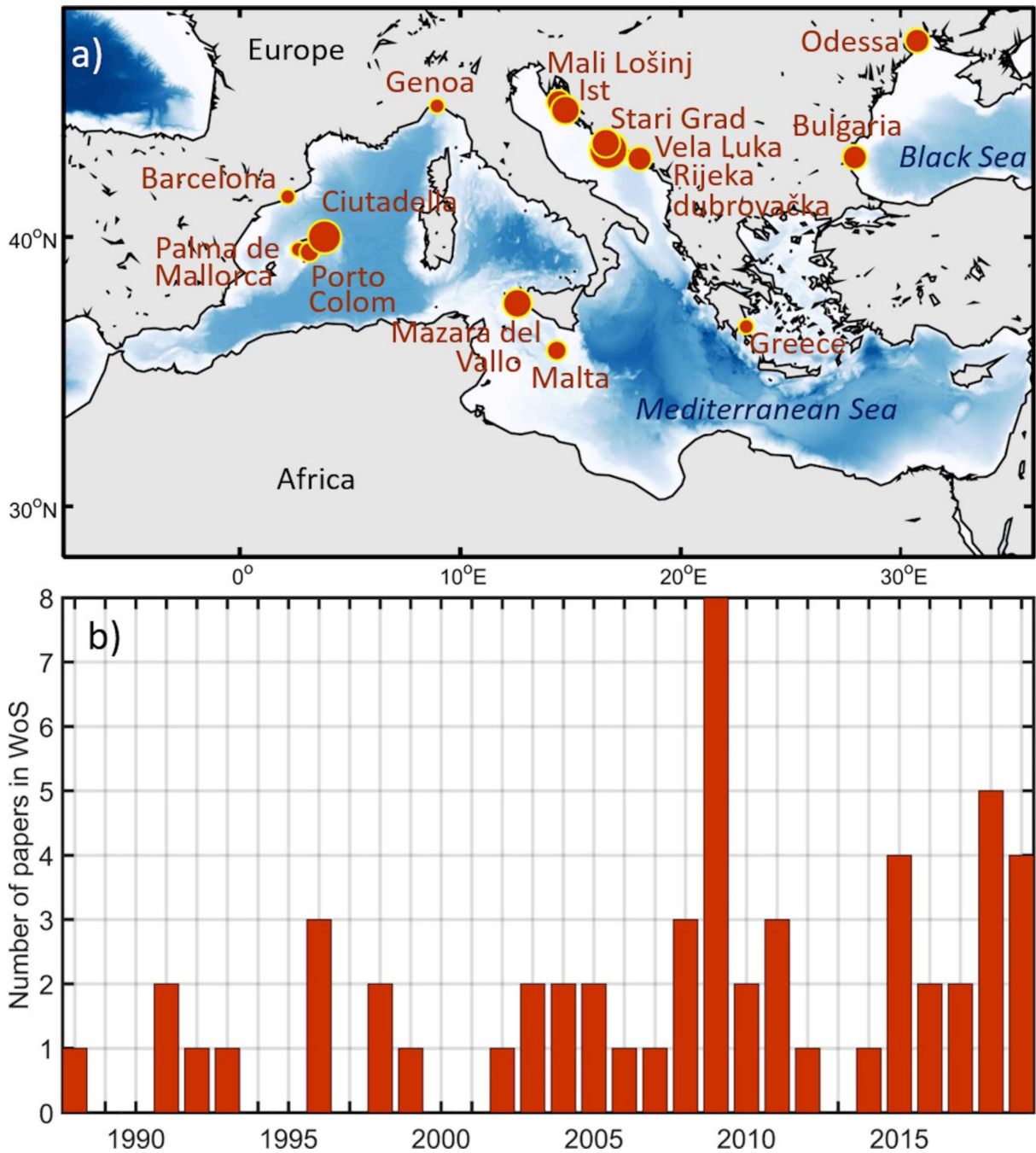
- 1902
- 1903
- 1904
- 1905
- 1906

Figure 2. Announcement of public works provided by local authorities the day after the 21 June 1978 Vela Luka meteotsunami (reproduced from Vučetić and Barčot, 2008).



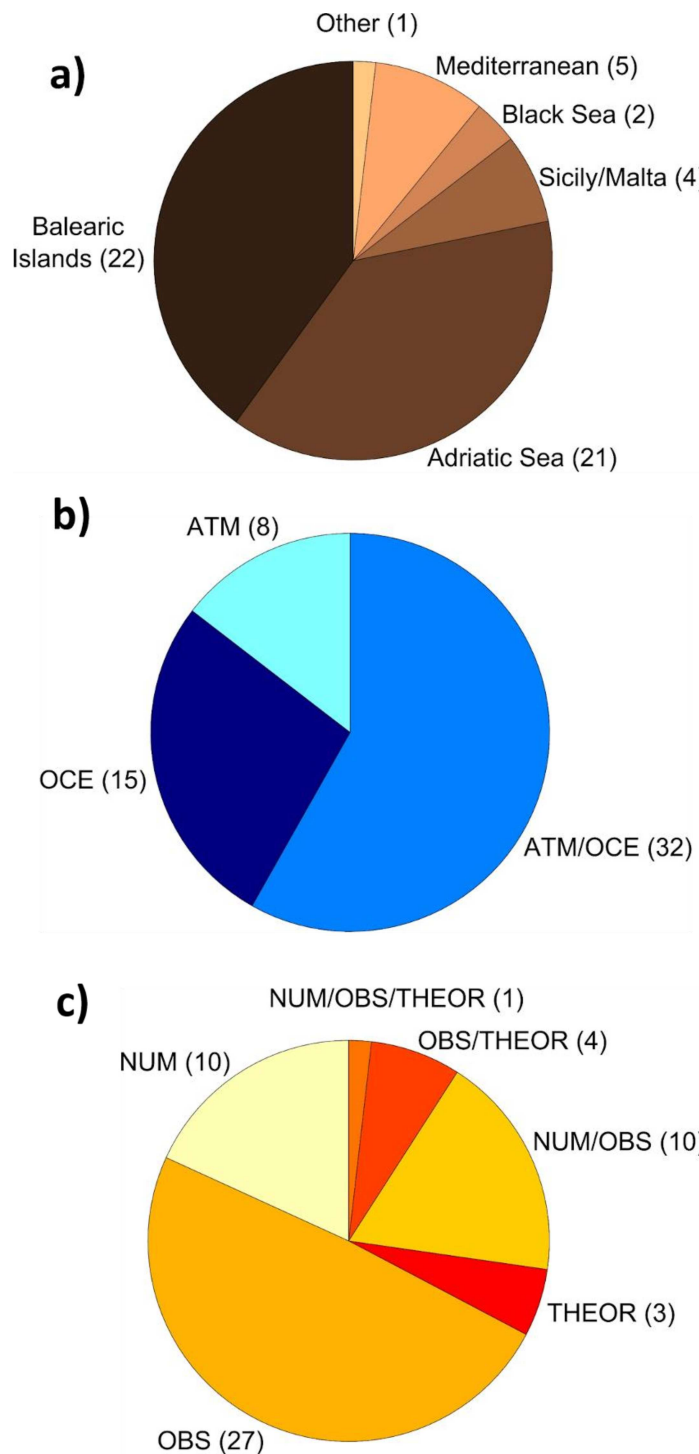
1907
1908
1909
1910
1911

Figure 3. Ciutadella harbour view taken during the 21st June 1984 rissaga event (courtesy of Josep Gornes).



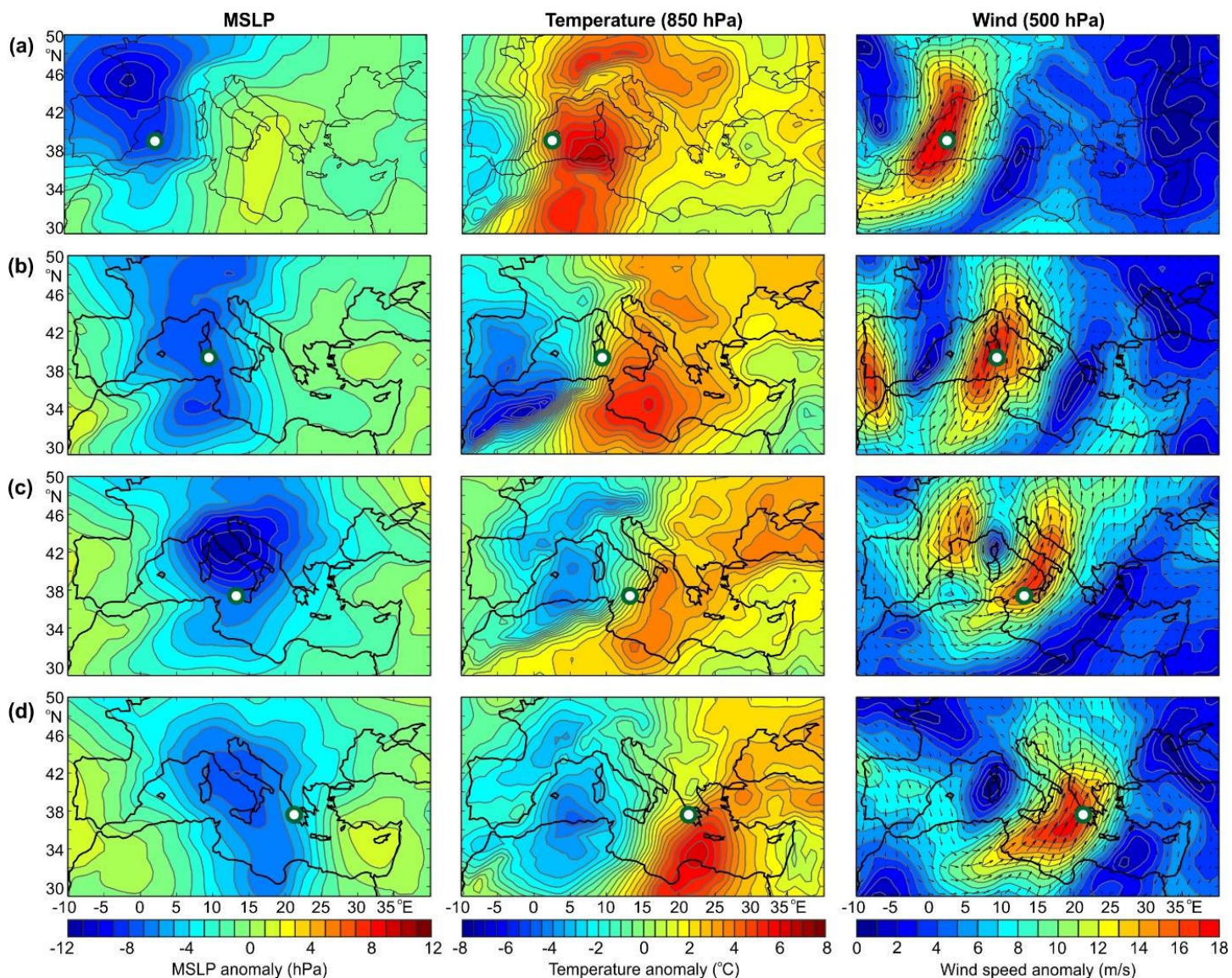
1912
1913
1914
1915
1916
1917
1918

Figure 4. (a) Meteor tsunami hot spots (red circles) in the Mediterranean and Black Sea as documented in the research literature; and (b) number of Mediterranean and Black Sea meteor tsunami papers published in Web of Science per year. The size of the circle is proportional to the observed or eyewitnessed wave height.

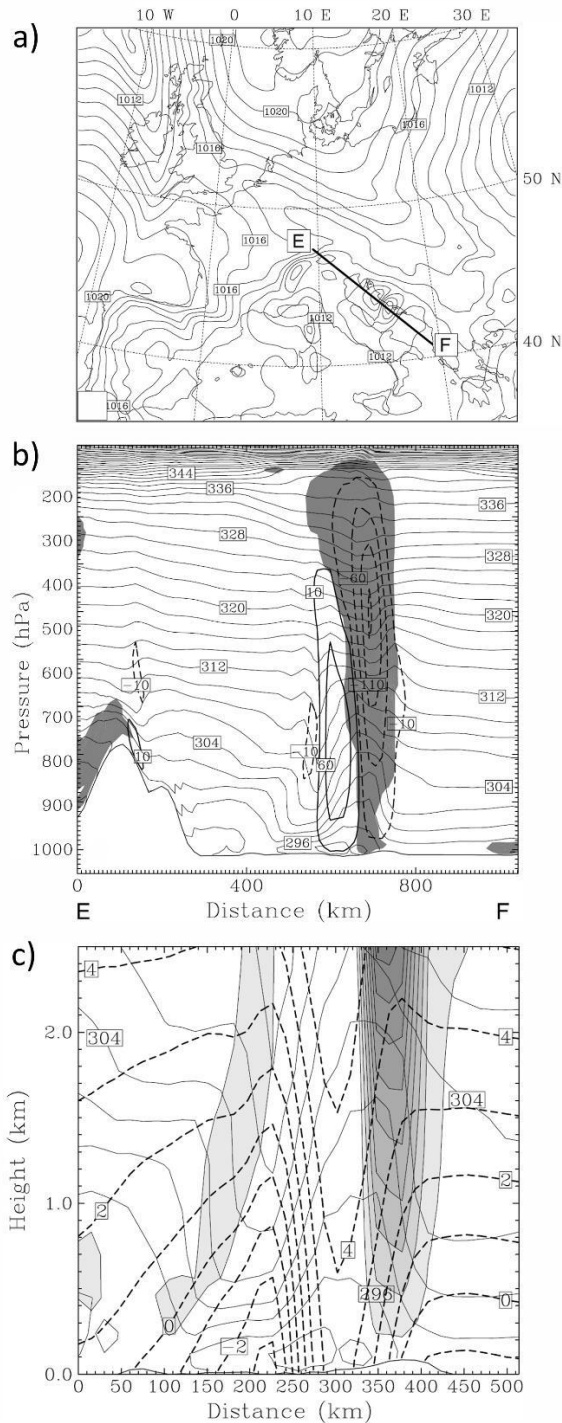


1919
1920
1921
1922
1923
1924
1925
1926
1927

Figure 5. Number of meteotsunami papers published in Web of Science categorized by (a) region of interest (Mediterranean stands for papers examining at least two regions or the whole basin), (b) studied process – atmospheric (ATM), ocean (OCE) or ocean-atmosphere (ATM/OCE) and (c) type of investigation – observational (OBS), numerical modelling (NUM), analytical modelling (THEOR) or combinations (NUM/OBS/THEOR).

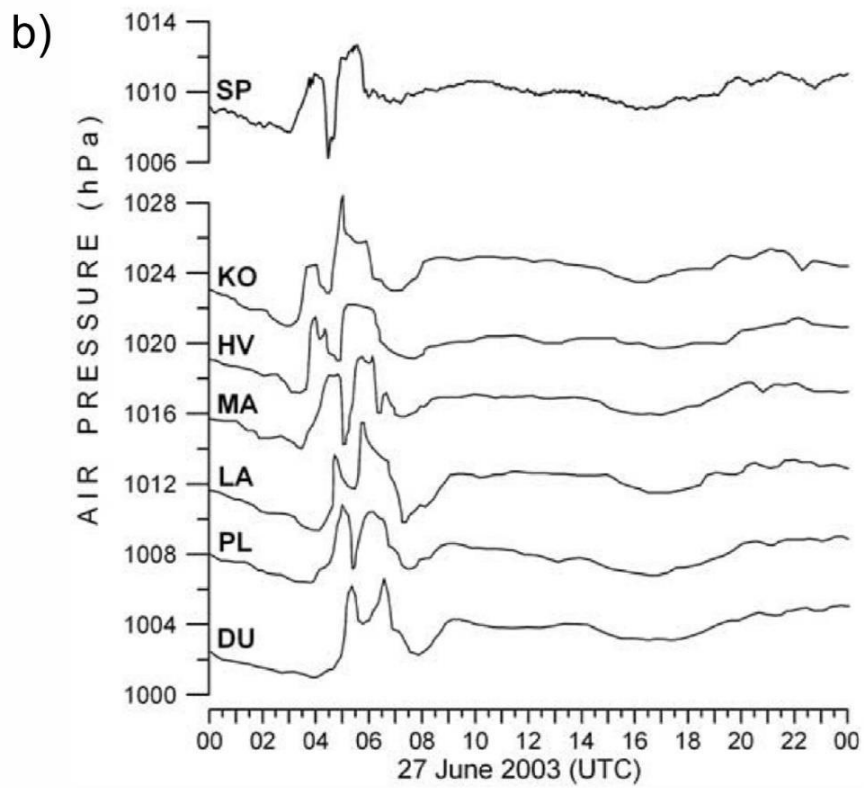
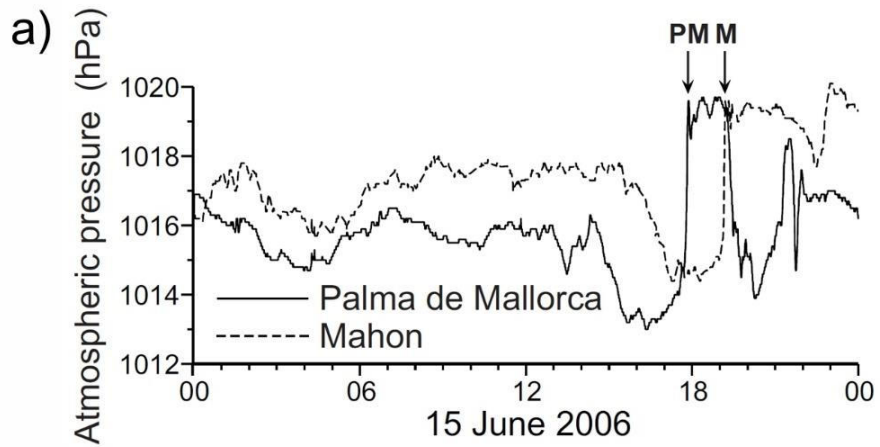


1929
 1930 Figure 6. Common synoptic patterns conducive for the observed Mediterranean high-
 1931 frequency sea level oscillations: mean sea level pressure (MSLP) anomaly, temperature at
 1932 850 hPa anomaly, and wind anomaly at 500 hPa averaged over selected events measured at
 1933 (a) Palma de Mallorca, (b) Cagliari, (c) Porto Empedocle and (d) Katakolo tide gauge stations.
 1934 Twelve high-frequency sea level oscillation events, 6 in each season (May–October,
 1935 November–April), are selected per quoted station between 2008 and 2014, with the full info
 1936 on events listed by Šepić et al. (2015c). The anomaly has been computed as the difference
 1937 between the actual synoptic field and the climatological synoptic field for the month in
 1938 which the event occurred. The figure is reproduced from Šepić et al. (2015c).
 1939



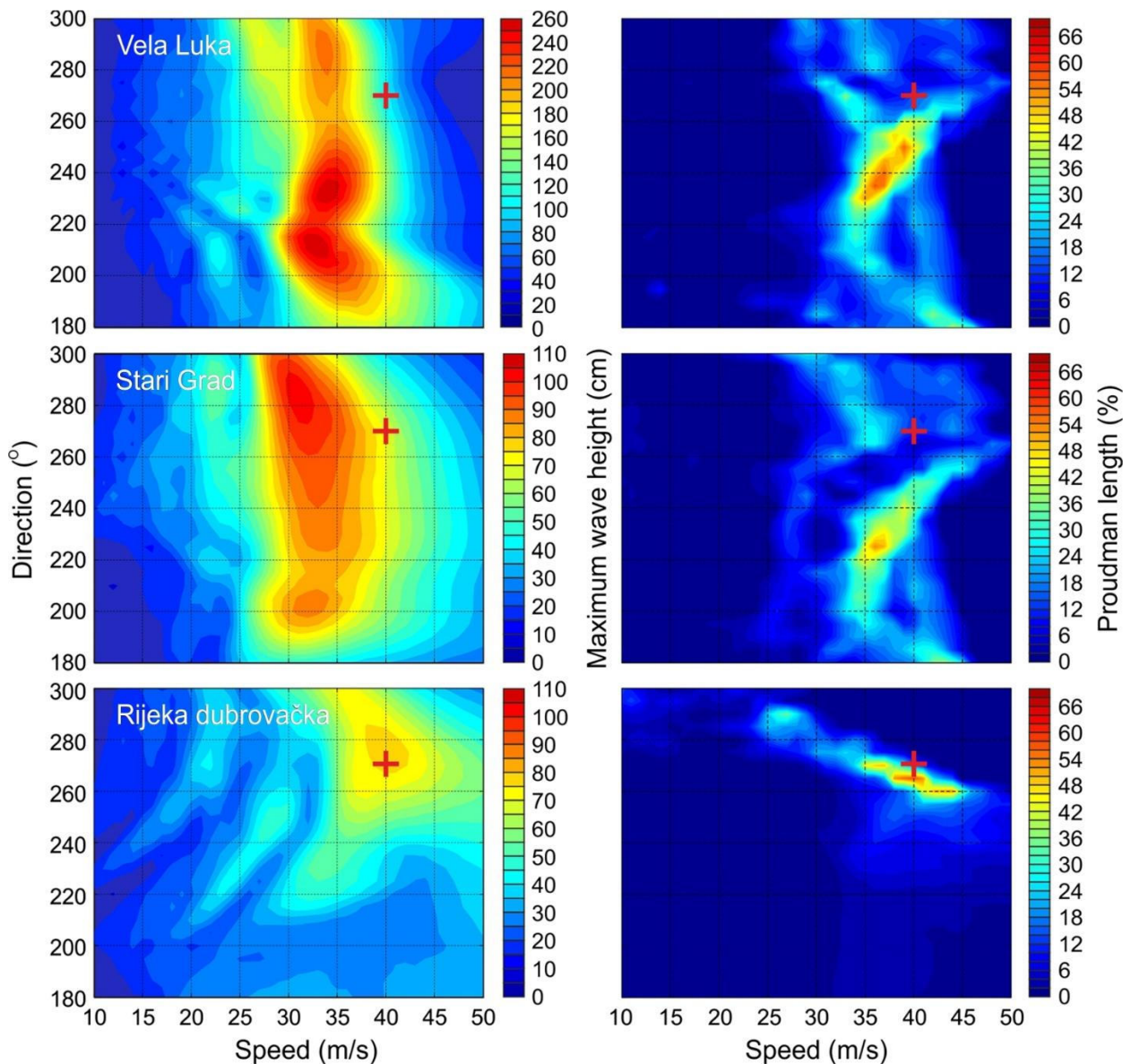
1940
 1941
 1942
 1943
 1944
 1945
 1946
 1947
 1948
 1949

Figure 7. Results of the numerical modelling exercise in reproduction of the 2003 middle Adriatic meteotsunami event: (a) mean sea level pressure and (b) vertical cross-section of potential temperature, cloud water/ice mixing ratio (shaded above 0.005 g/kg) and vertical velocity (contours of 10, 60 and 110 dPa/s, negative values standing for updrafts and are dashed), and (c) zoomed potential temperature (solid lines, interval 2 K), pressure perturbation (dashed lines, interval 1 hPa), and vertical velocity (shaded above 5 cm/s, contour interval 10 cm/s), all on 27 June 2003 at 02 UTC. The figures are taken from Belušić et al. (2007).



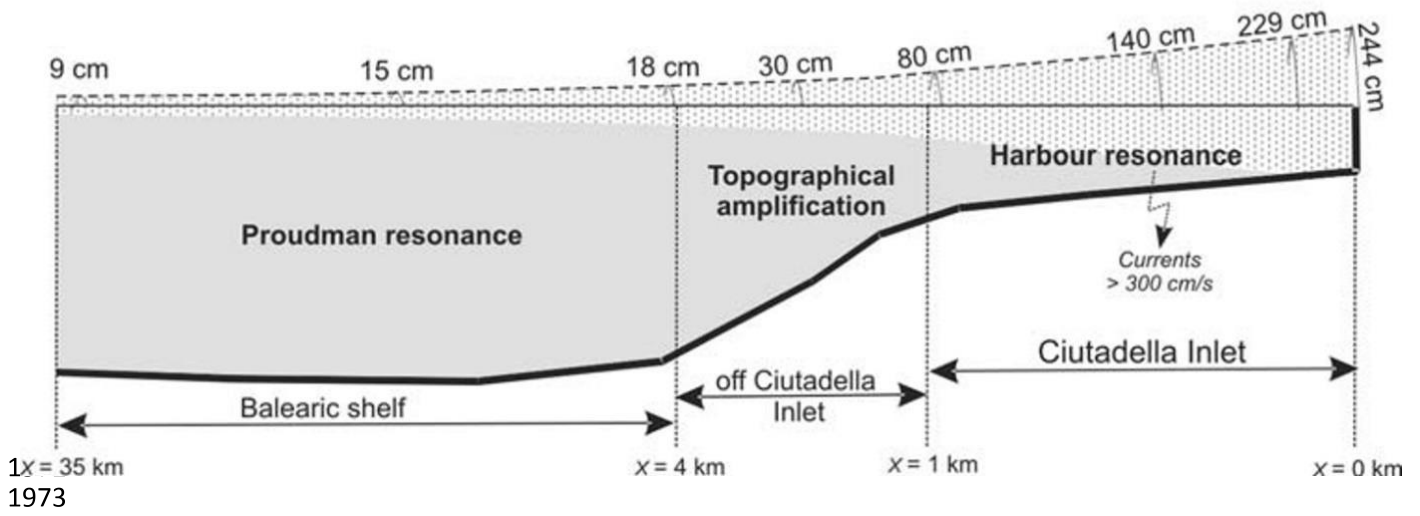
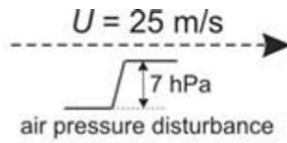
1950
1951
1952
1953
1954
1955
1956
1957
1958

Figure 8. Air pressure series measured at microbarograph stations (a) during the 15 June 2006 Balearic meteotsunami (after Monserrat et al. 2006), and (b) during the 27 June 2003 Adriatic meteotsunami (after Vilibić et al. 2004). PM, M, SP, KO, HV, MA, LA, PL and DU stand for Palma de Mallorca, Mahon, Split, Komiža, Hvar, Makarska, Lastovo, Ploče and Dubrovnik, respectively.



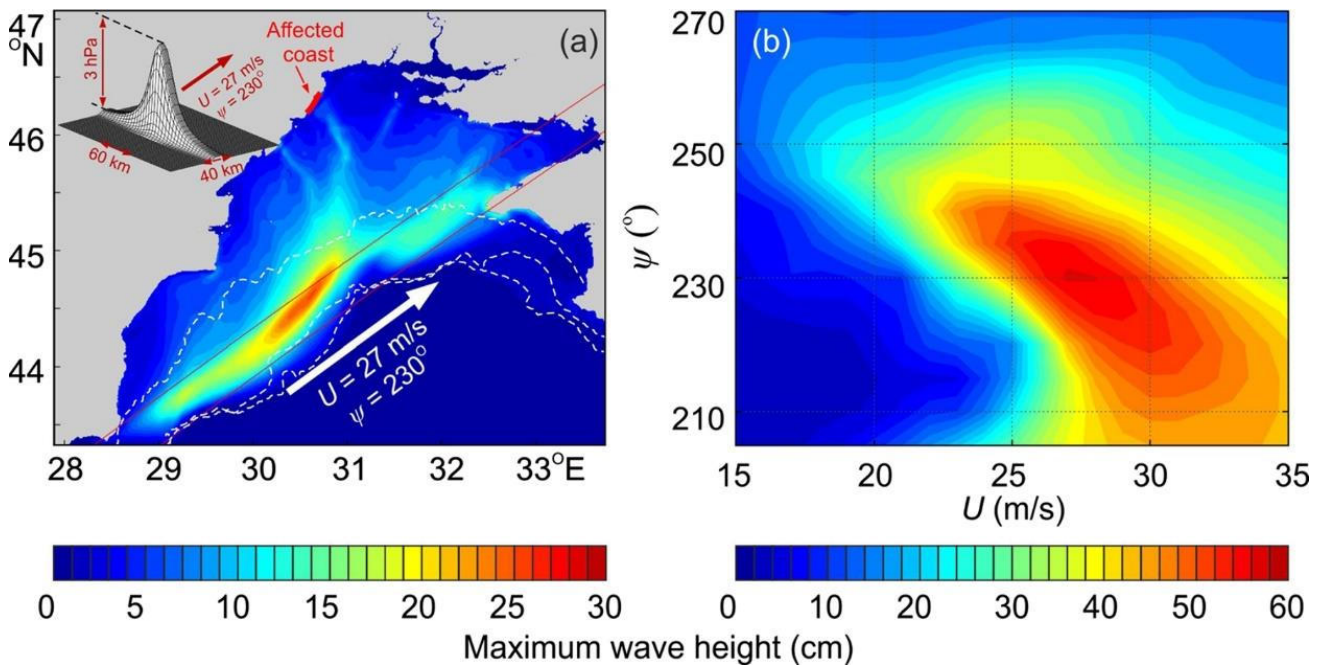
1959
1960
1961
1962
1963
1964
1965
1966
1967
1968
1969
1970
1971

Figure 9. Sensitivity modelling study of the 25 June 2014 Adriatic meteotsunami: (a) maximum wave heights obtained for the tops of Vela Luka, Stari Grad and Rijeka dubrovačka bays for a set of experiments forced by a box-car air pressure disturbance. (b) Proudman length at the tops of Vela Luka, Stari Grad and Rijeka dubrovačka bays, defined as a percentage of total length over which a disturbance travelled, and for which $0.95 < Fr < 1.05$ is valid, where Fr is Froude number defined as ratio between the speed of atmospheric disturbance and long ocean waves. Red plus signs mark maximum wave height and Proudman length as obtained in experiment forced by a disturbance propagating with speed and direction estimated from measurements ($u = 40$ m/s, $c = 270^\circ$). The figure is reproduced from Šepić et al. (2016b).



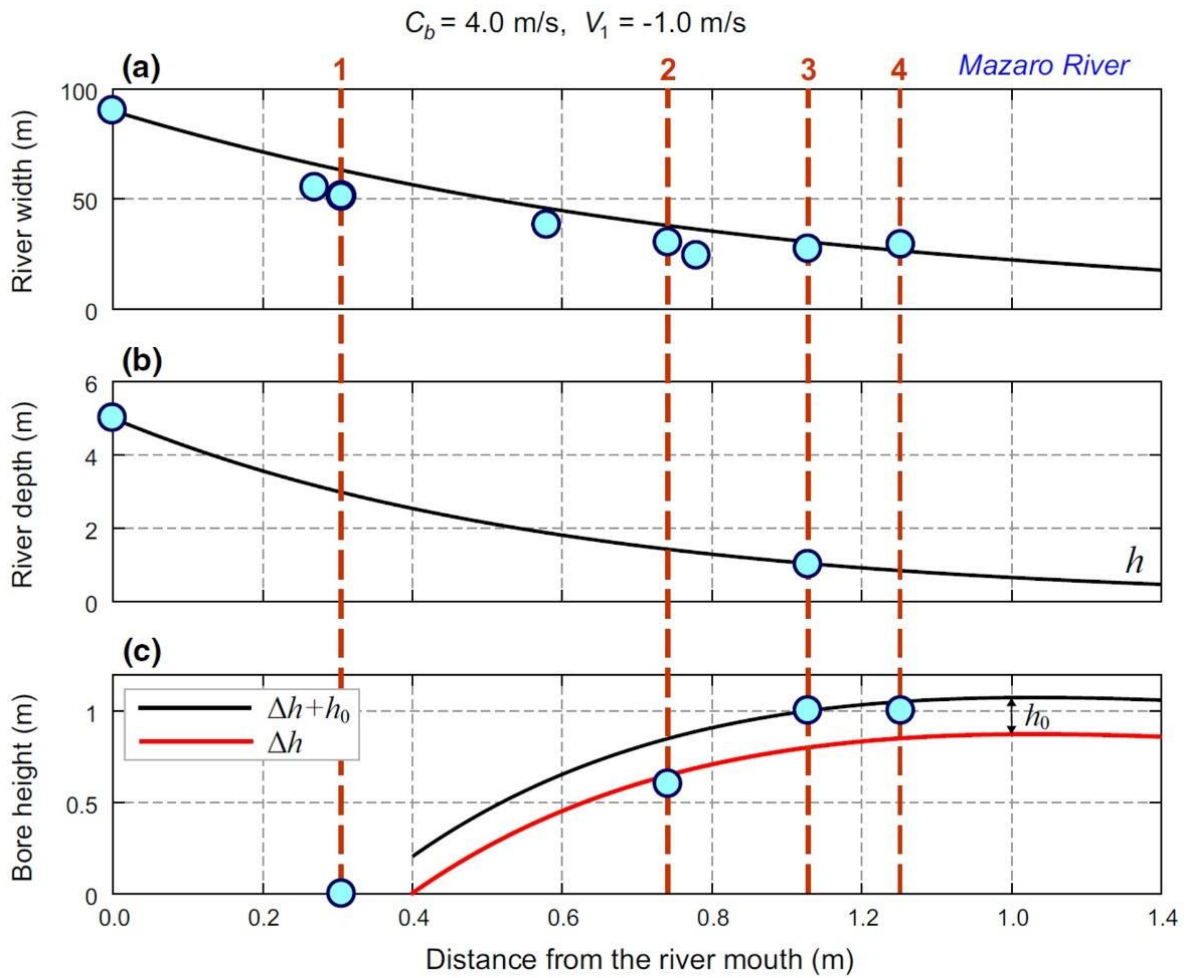
1973
1974 Figure 10. A sketch illustrating the physical mechanisms responsible for the formation of the
1975 destructive rissaga on 15 June 2006 in Ciutadella Harbour, Menorca Island (after Vilibić et al.
1976 2008).

1977
1978
1979



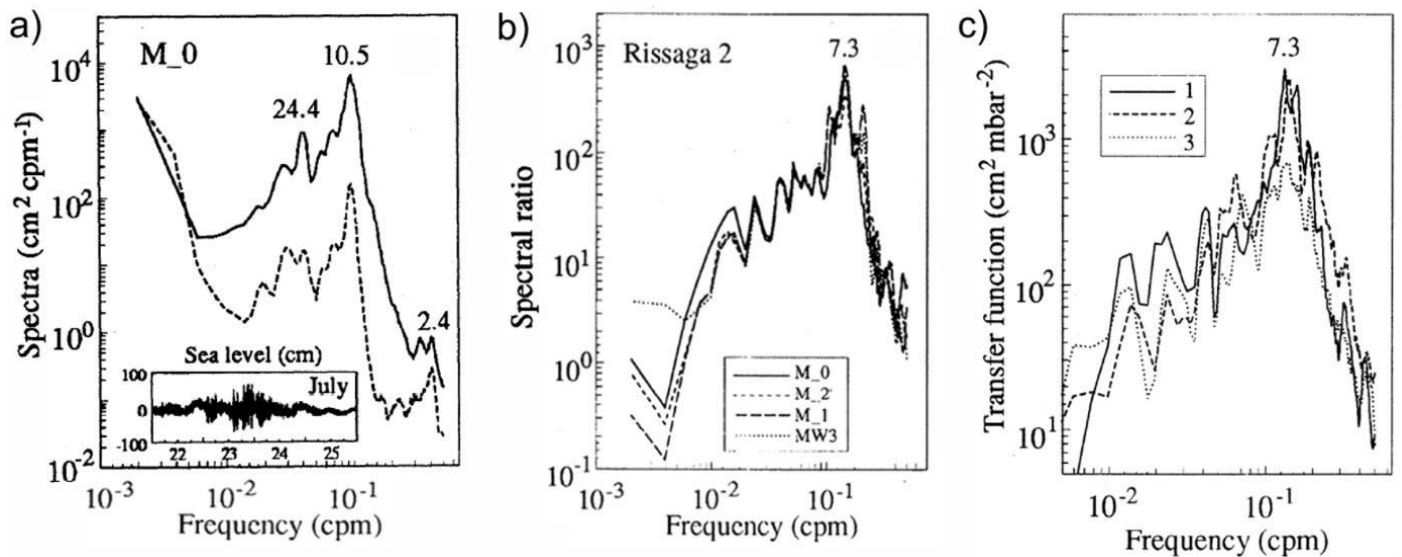
1980
1981
1982 Figure 11. Topographical channelling of the meteotsunami waves: (a) maximum modelled
1983 wave height across western Black Sea model domain for experiment in which an air pressure
1984 disturbance propagates with a speed of 27 m/s and a direction of 230°, and (b) maximum
1985 simulated wave heights at Odessa as function of speed, U , and direction, ψ , of the
1986 propagating air pressure disturbance (after Šepić et al. 2018a).

1987



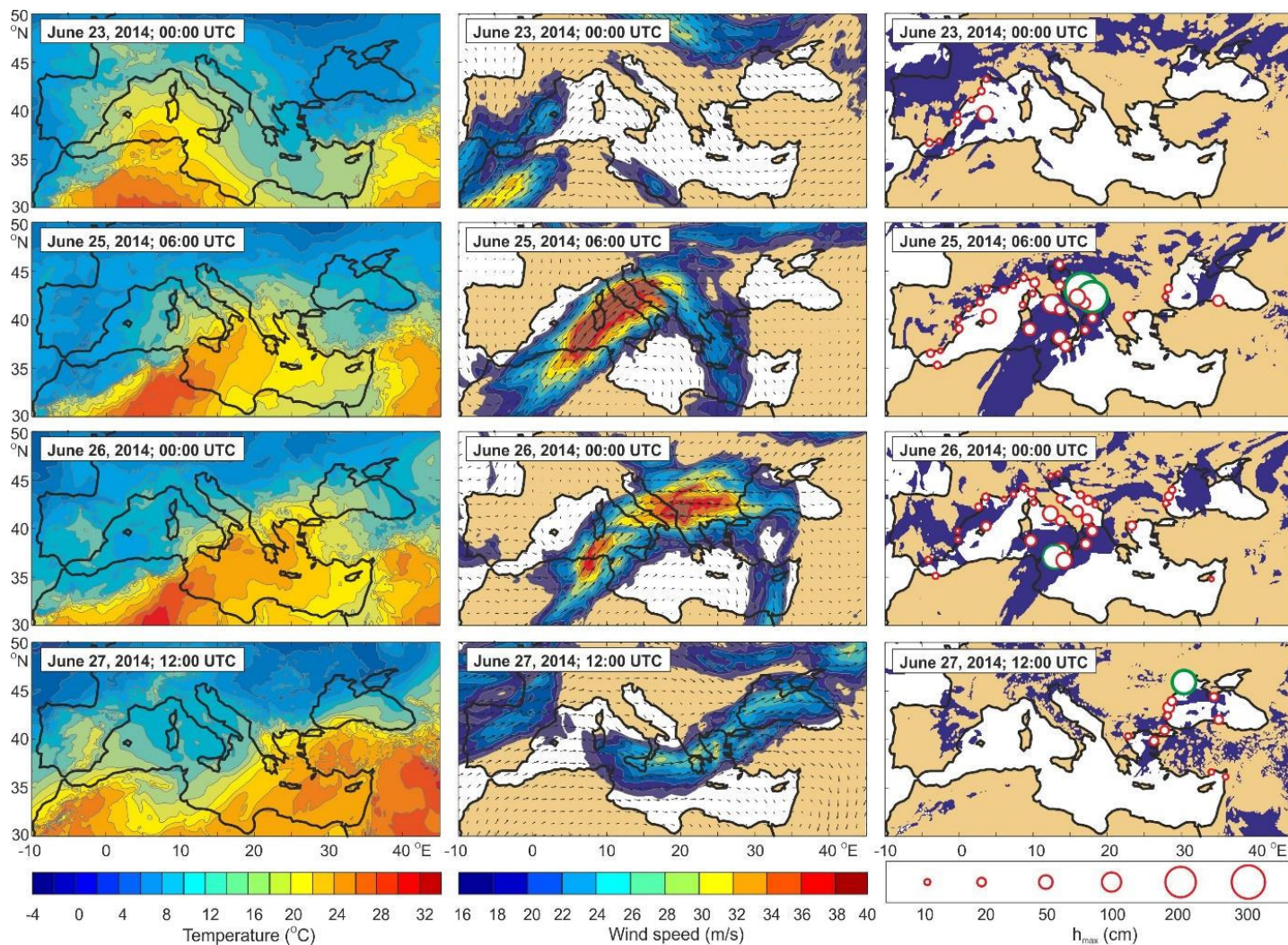
1988
 1989
 1990
 1991
 1992
 1993
 1994
 1995
 1996
 1997
 1998
 1999

Figure 12. Approximate profiles of the Mazaro River (a) width and (b) depth; (c) estimated meteobore heights. Light blue circles denote data available on the river bathymetry and from video footages (the latter are indicated by vertical dashed red lines). Black and red solid lines indicate meteobore heights estimated by the model with and without incoming open-sea wave height (h_0), respectively (after Šepić et al. 2018b).



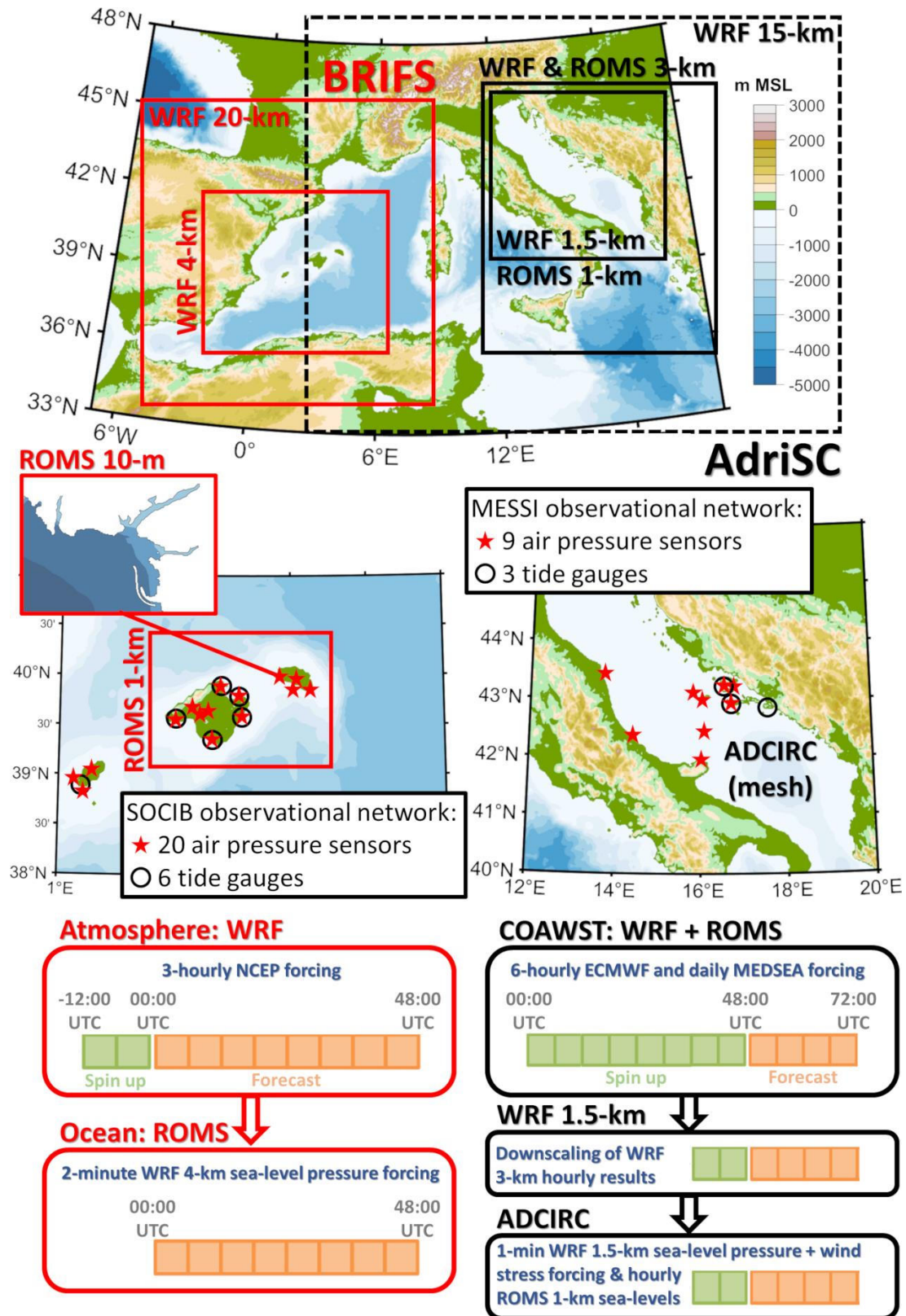
2001
 2002
 2003
 2004
 2005
 2006
 2007
 2008
 2009
 2010
 2011

Figure 13. (a) Sea level spectra at Ciutadella (Menorca Island) computed during the meteotsunami of 22-25 July 1997 (solid line) and during a background period (dashed line), (b) event-vs-background spectral ratio for the same meteotsunami event computed at two points in Ciutadella (M_0 and M_2), in nearby inlet Platja Gran (M_1) and over the external platform (MW3) , and (c) atmosphere-ocean transfer function for three different meteotsunami events observed during summer 1997 (after Monserrat et al. 1998).



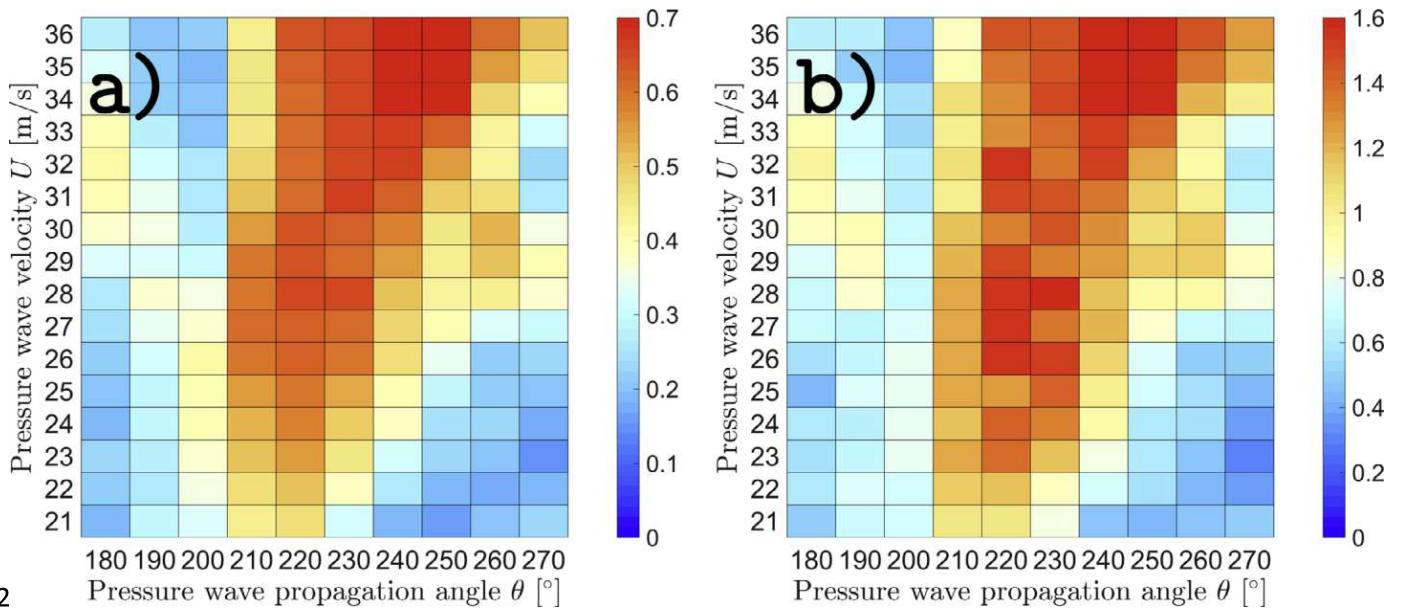
2013
 2014
 2015
 2016
 2017
 2018
 2019
 2020
 2021
 2022
 2023

Figure 14. The sequence of meteotsunamigenic synoptic patterns conjoined with high-frequency sea level oscillations (reproduced from Šepić et al. 2015a). Left panel: temperature at 850 hPa; middle panel: wind speed and direction at 500 hPa; and right panel: the dynamically unstable atmospheric layers (collared denotes $Ri < 0.25$) overlaid by circles showing the maximum height of high-frequency (periods < 3 h) sea level oscillations; the red circles denote measured wave heights; the green circles denote wave heights estimated from videos and eyewitness reports.



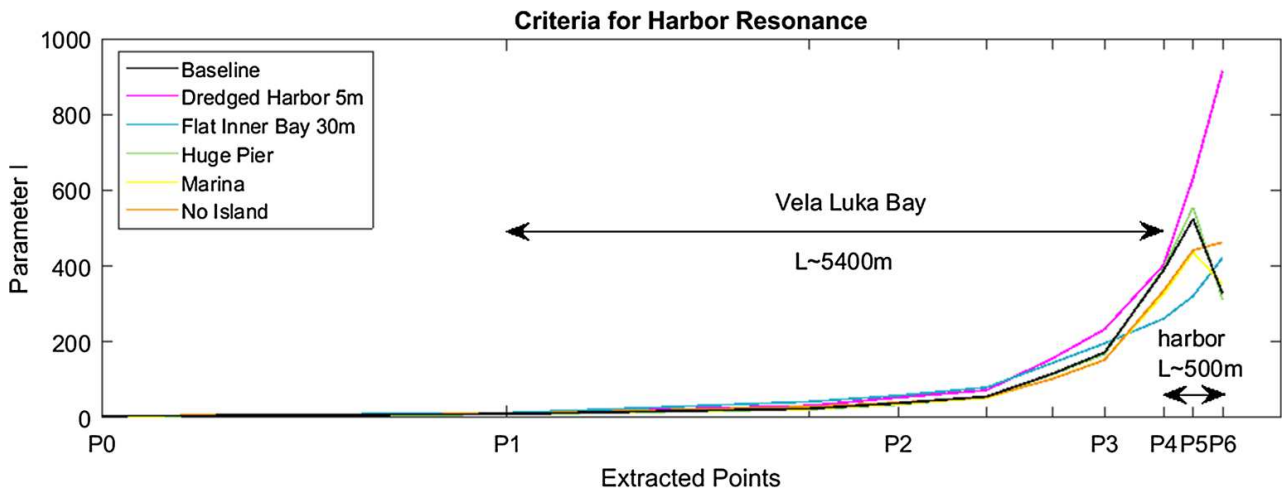
2024
 2025
 2026
 2027
 2028
 2029
 2030

Figure 15. Existing meteotsunami monitoring and forecasting systems in the Mediterranean Sea: BRIFS (in red) associated with the SOCIB observational network in the Balearic Islands and AdriSC forecast system (in black) associated with the MESSI observational network in the Adriatic Sea.



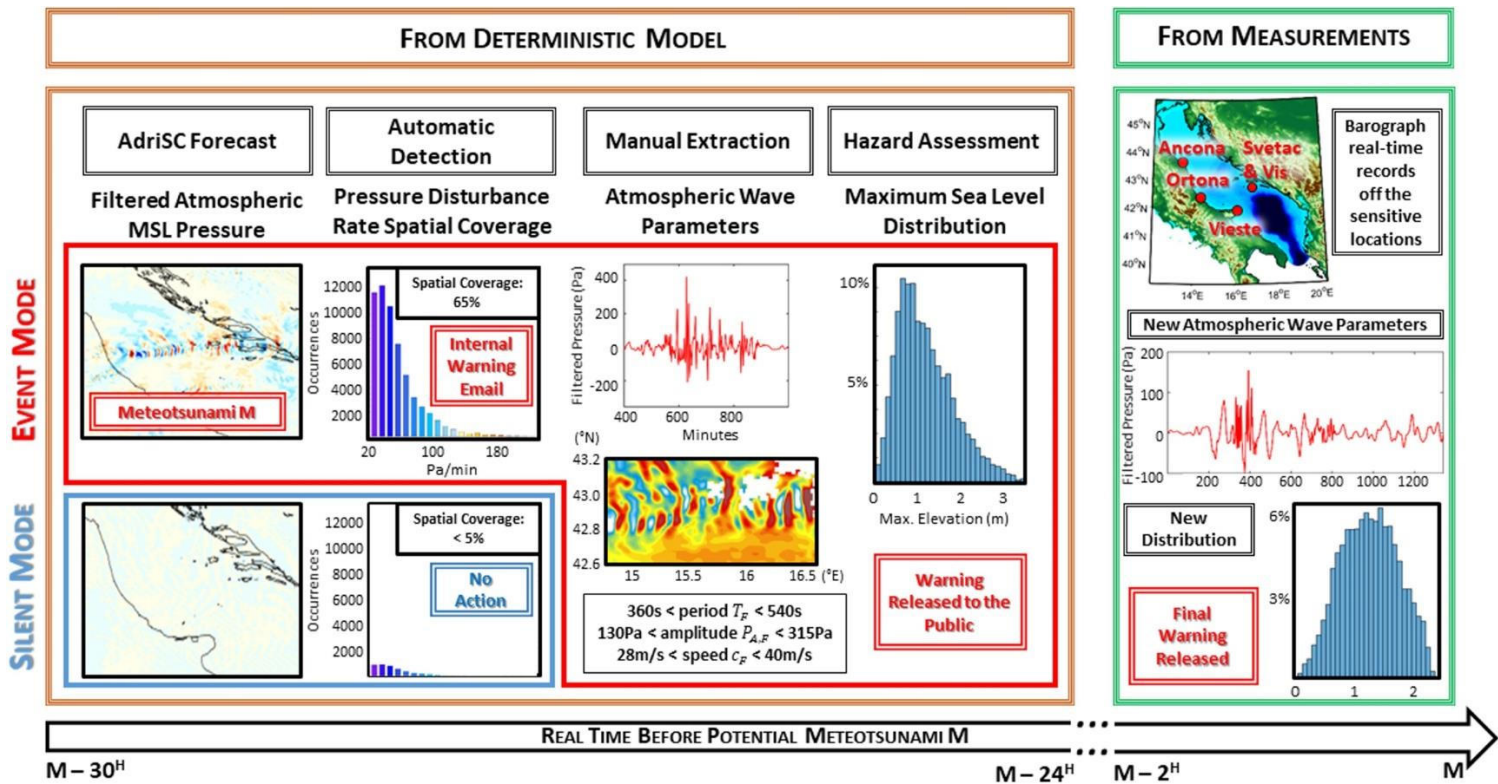
2
2032
2033
2034
2035
2036
2037
2038
2039

Figure 16. Dependence of the maximum generated sea surface anomaly (m) on the forcing gravity wave incident angle θ and speed U (a) outside and (b) inside Ciutadella Harbour (after Ličer et al. 2017).



2040
2041
2042
2043
2044
2045
2046

Figure 17. Variation of the re-calculated amplification factor (I) along the Vela Luka Bay (with P_0 located at the entrance of the bay and P_4 to P_6 inside of the harbour) for different geomorphologies (after Denamiel et al. 2018).



M - 30^H

M - 24^H M - 2^H

M

2048

2049

2050

2051

2052

2053

2054

2055

2056

2057

2058

2059

2060

2061

2062

2063

2064

2065

Figure 18. Operational meteotsunami hazard forecast within the Croatian Meteotsunami Early Warning System, based on atmospheric pressure field input from both (1) the deterministic model results (brown box) and (2) the measurements (green box). Every day, at least 30 hr before any meteotsunami event, the high-pass filtered pressure is extracted from the AdriSC forecast and used to automatically detect meteotsunamis by checking the spatial coverage of the values above 20 Pa per 4-min interval of the maximal pressure temporal rate. If this coverage is below 5%, then no meteotsunami is forecasted (blue box)—“silent” warning mode, otherwise a potential meteotsunami M is foreseen to occur (red box)—“event” warning mode, and an email is sent to the AdriSC team. At least 24 hr before the potential meteotsunami M occurs, the first forecast of hazard assessment is derived from the stochastic surrogate model used with ranges of pressure wave parameters manually extracted from the modelled filtered pressure. Finally, when the real-time observations become available, the hazard assessment is updated with new parameters extracted from the measurements (after Denamiel et al. 2019b).